

Interaction and Identification of the Meson-Baryon molecules

D. P. Rathaud* and Ajay kumar Rai†

Department of Applied Physics, Sardar Vallabhbhai National Institute of Technology, Surat, Gujarat-395007, India.

(Dated: March 3, 2022)

The challenges with the molecular model of the multi-quark systems are the identification of the hadronic molecules and the interaction between two color neutral hadrons. We study the di-hadronic molecular systems with proposed interaction potential as s-wave one boson exchange potential along with Screen Yukawa-like potential, and arrived with the proposal that within hadronic molecule the two color neutral hadrons experience the dipole-like interaction. The present study is the continuation of our previous study [1]. With the proposed interaction potential, the mass spectra of $\Sigma_s K^*$, $\Sigma_c K^*$, $\Sigma_b K^*$, $\Sigma_s D^*$, $\Sigma_c D^*$, $\Sigma_b D^*$, $\Sigma_s B^*$, $\Sigma_c B^*$, $\Sigma_b B^*$, $\Xi_s K^*$, $\Xi_c K^*$, $\Xi_b K^*$, $\Xi_s D^*$, $\Xi_c D^*$, $\Xi_b D^*$, $\Xi_s B^*$, $\Xi_c B^*$, $\Xi_b B^*$ meson-baryon molecules are predicted. The Weinberg compositeness theorem which provides clue for the compositeness of the state is used for determination of the scattering length and effective range. The present study predicts $P_c(4450)$ pentaquark state as $\Sigma_c D^*$ molecule with $I(J^P) = \frac{1}{2}(\frac{3}{2}^-)$. The formalism also predicts some very interesting open as well as hidden flavour near threshold molecular pentaquark states.

I. INTRODUCTION

The multi-quark states come again in the focus of interest, with the discovery of the two new observations $P_c(4380)^+$ and $P_c(4450)^+$, reported by LHCb Collaboration in 2015 [2]. Both of these states could be potential candidate of the pentaquark state. The subject of the non conventional hadrons (exotic hadrons) has been speculated since the beginning of the quark model [3, 4]. The idea of non conventional baryon composed of four quark and an anti-quark was introduced in refs. [5, 6], while the name pentaquark was devised by Lipkin [6].

The first claim of the pentaquark was in 2003 by LEPS Collaboration, as a Θ_s^+ state, with suggesting the minimal quark content $uudd\bar{s}$, having the strangeness $S=+1$ [7]. After this claim, two other experimental groups DIANA [8] and CLAS [9] were found positive signatures for Θ_s^+ . With following these positive motivation, charm and bottom analogue of Θ_s^+ were predicted as Θ_c and Θ_b . Meanwhile in 2004, H1 collaboration at HERA reported the observation of the Θ_c [10]. However, some experiments reported negative results regarding the status of Θ_s^+ , Θ_c and Θ_b [11–15]. Even, some recent experimental efforts, such as E19 Collaboration at J-PARC for the search of Θ^+ [16] and ALICE collaboration for the $\phi(1869)$ pentaquark [17], reported negative results. Within this situation, LHCb in 2015 has boosted the interest for the search of the multi-quark states and their studies by reported promising hidden charm pentaquark states, named as $P_c(4380)^+$ with mass $4380 \pm 8 \pm 29$ MeV and width $205 \pm 18 \pm 86$ MeV, respectively along with another state $P_c(4450)^+$ with mass $4449.8 \pm 1.7 \pm 2.5$ MeV and a narrow width $39 \pm 5 \pm 19$ MeV. The spin-parity of these two states are $\frac{3}{2}$ are $\frac{5}{2}$ with opposite parity have

been proposed [2]. The definite spin and parity for both of these states has not yet been defined.

These controversial history regarding the search and study of multi-quark states, for instant pentaquark states, made the subject more fascinating from both theoretical and experimental point of view. Since various theoretical efforts have been made to understand the properties of these states, such as compact pentaquarks model [18–21], meson-baryon molecules [22–26], topological soliton model [27], kinematic rescattering effects [28–31], cups like effect [], hadroquarkonia model [32] etc. One can find some brief review articles on multi-quark states including pentaquarks in Refs. [33–36], for the review on hadronic molecules, one should see ref. [37] and references therein. These theoretical efforts suggested that the study of the multi-quark states required more attention to reveal the information of their substructure and nature.

The present article focus on the molecular picture of the pentaquark (meson-baryon bound states) states. The work of this article is the continuation of our previous study presented in ref. [1]. In [1], the results of the dimesonic systems have been presented.

The aim of our study is to attempt two challenges of the molecular model: (i) interaction between two color neutral hadrons (ii) identification of the hadronic molecules from confined states. The interaction between two color neutral states is largely unknown. The various interaction potentials have been used to explain such hadronic molecular structure [38–43]. The hadronic molecules should close to the s-wave. Therefore, we proposed the interaction potential as s-wave One Boson Exchange Potential where the range of the force is proportional to the inverse mass of the exchange mesons. We notice that the s-wave OBE potential could not gain sufficient attractive strength for bound state, thus, we have added a screen Yukawa-like potential for additional attractive strength. This additional potential is added with a proposal that the two color neutral states experienced dipole-like interaction. The potential parameters of the s-wave OBE and screen Yukawa-like potential are fitted

* Also at Department of Applied Physics, Sardar Vallabhbhai National Institute of Technology, Surat, Gujarat-395007, India.

† dharmeshphy@gmail.com

to get experimental binding energy of the deuteron. The screen parameter 'c' of screen Yukawa-like potential is the only free parameter of the model and only fitted for deuteron, while it is taken as a fixed parameter for all di-hadronic calculation. With this model, the results and analysis of the meson-baryon molecular systems are presented in this article. The characteristic contributory nature of the individual s-wave meson exchange and effective s-wave OBE potential are presented in result and discussion section. The second prerequisite of hadronic molecule model, identification of the hadronic molecule, we have adopted the Weinberg's compositeness theorem and results of scattering length (a_s) and effective range (r_e) are extracted for attempted meson-baryon molecular states.

The article is organized as follows: after the brief introduction, theoretical framework and the model is introduced in the section-II, after that the results of the mass spectra of meson-baryon molecular systems are presented in section-III. The compositeness theorem and the results of the scattering length and effective range for attempted systems are presented in section-IV, finally the summary and conclusion is presented in the last section-V.

II. THEORETICAL FRAMEWORK

The Hamiltonian of di-hadronic molecule is given by

$$H = \sqrt{P^2 + m_d^2} + \sqrt{P^2 + m_b^2} + V_{hh}(r_{db}) \quad (1)$$

m_d and m_b are the masses of constituents and P is the relative momentum of two hadrons while the $V_{hh}(r_{db})$ is the inter-hadronic interaction potential. In the variational scheme, we have used the hydrogenic trial wave function to determine the expectation value of the Hamiltonian.

The di-hadronic interaction potential is given by

$$V_{hh}(r_{db}) = V_{OBE}(r_{db}) + V_Y(r_{db}) \quad (2)$$

the term $V_Y(r_{db})$ is screen Yukawa-like potential and V_{OBE} is the s-wave One Boson Exchange (OBE) potential.

The additional phenomenological screen Yukawa-like potential is used along with s-wave OBE potential to get sufficient attractive strength for bound state. For use of such potential, we have taken an approximation that two

color neutral hadrons experienced the dipole-dipole like interaction, where it could be either permanent dipole or induced dipole in which the latter one is weakest. The screen Yukawa-like potential expressed as

$$V_Y = -\frac{k_{mol}}{r_{db}} e^{-\frac{c^2 r_{db}^2}{2}} \quad (3)$$

here, c is a screen fitting parameter of the potential while k_{mol} is the residual running coupling constant, namely

$$k_{mol}(M^2) = \frac{4\pi}{(11 - \frac{2}{3}n_f) \ln \frac{M^2 + M_B^2}{\Lambda_Q^2}} \quad (4)$$

where $M=2m_d m_b / (m_d + m_b)$, m_d and m_b are constituent masses, $M_B=1$ GeV, Λ_Q is QCD scale parameter, respectively. The term n_f is number of flavour [44, 45]. This effective coupling constant has introduced to incorporate the asymptotic behavior at short distance as well as to reduce the free parameter of the model.

The light mesons under consideration for the OBE Potential are as follows [38]:

Pseudoscalar meson (ps) = π, η

Scalar meson (s) = σ, δ (also known as a_0)

Vector meson (v) = ω, ρ .

The OBE potential is sum of the all one meson exchange, namely

$$V_{OBE} = V_{ps} + V_s + V_v \quad (5)$$

The OBE potential with finite size effect due to extended structure of the hadrons can be expressed as [38]

$$V_\alpha(r_{db}) = V_\alpha(m_\alpha, r_{db}) - F_{\alpha 2} V_\alpha(\Lambda_{\alpha 1}, r_{db}) + F_{\alpha 1} V_\alpha(\Lambda_{\alpha 2}, r_{db}) \quad (6)$$

where $\alpha = \pi, \eta, \sigma, \delta, \omega$ and ρ mesons, while

$$\Lambda_{\alpha 1} = \Lambda_\alpha + \epsilon \quad \text{and} \quad \Lambda_{\alpha 2} = \Lambda_\alpha - \epsilon$$

$$F_{\alpha 1} = \frac{\Lambda_{\alpha 1}^2 - m_\alpha^2}{\Lambda_{\alpha 2}^2 - \Lambda_{\alpha 1}^2} \quad \text{and} \quad F_{\alpha 2} = \frac{\Lambda_{\alpha 2}^2 - m_\alpha^2}{\Lambda_{\alpha 2}^2 - \Lambda_{\alpha 1}^2} \quad (7)$$

the subscript α tends for mesons ($\pi, \eta, \sigma, \delta, \omega$ and ρ) $\epsilon/\Lambda_\alpha \ll 1$, thus $\epsilon=10$ MeV is an appropriate choice.

Hence, the individual meson exchange potential with finite size effect can be expressed as [38]

$$V_{ps}(r_{db})_F = \frac{1}{12} \left[\frac{g_{\pi qq}^2}{4\pi} \left\{ \left(\frac{m_\pi}{m} \right)^2 \frac{e^{-m_\pi r_{db}}}{r_{db}} - (F_{\pi 2}) \left(\frac{\Lambda_{\pi 1}}{m} \right)^2 \frac{e^{-\Lambda_{\pi 1} r_{db}}}{r_{db}} + (F_{\pi 1}) \left(\frac{\Lambda_{\pi 2}}{m} \right)^2 \frac{e^{-\Lambda_{\pi 2} r_{db}}}{r_{db}} \right\} (\tau_d \cdot \tau_b) \right. \\ \left. + \frac{g_{\eta qq}^2}{4\pi} \left\{ \left(\frac{m_\eta}{m} \right)^2 \frac{e^{-m_\eta r_{db}}}{r_{db}} - (F_{\eta 2}) \left(\frac{\Lambda_{\eta 1}}{m} \right)^2 \frac{e^{-\Lambda_{\eta 1} r_{db}}}{r_{db}} + (F_{\eta 1}) \left(\frac{\Lambda_{\eta 2}}{m} \right)^2 \frac{e^{-\Lambda_{\eta 2} r_{db}}}{r_{db}} \right\} (\sigma_d \cdot \sigma_b) \right] \quad (8)$$

$$\begin{aligned}
V_s(r_{db})_F = & -\frac{g_{\sigma qq}^2}{4\pi} \left\{ m_\sigma \left[1 - \frac{1}{4} \left(\frac{m_\sigma}{m} \right)^2 \right] \frac{e^{-m_\sigma r_{db}}}{m_\sigma r_{db}} - F_{\sigma 2} \Lambda_{\sigma 1} \left[1 - \frac{1}{4} \left(\frac{\Lambda_{\sigma 1}}{m} \right)^2 \right] \frac{e^{-\Lambda_{\sigma 1} r_{db}}}{\Lambda_{\sigma 1} r_{db}} + F_{\sigma 1} \Lambda_{\sigma 2} \right. \\
& \left. \left[1 - \frac{1}{4} \left(\frac{\Lambda_{\sigma 2}}{m} \right)^2 \right] \frac{e^{-\Lambda_{\sigma 2} r_{db}}}{\Lambda_{\sigma 2} r_{db}} \right\} + \frac{g_{\delta qq}^2}{4\pi} \left\{ m_\delta \left[1 - \frac{1}{4} \left(\frac{m_\delta}{m} \right)^2 \right] \frac{e^{-m_\delta r_{db}}}{m_\delta r_{db}} - F_{\delta 2} \Lambda_{\delta 1} \left[1 - \frac{1}{4} \left(\frac{\Lambda_{\delta 1}}{m} \right)^2 \right] \right. \\
& \left. \frac{e^{-\Lambda_{\delta 1} r_{db}}}{\Lambda_{\delta 1} r_{db}} + F_{\delta 1} \Lambda_{\delta 2} \left[1 - \frac{1}{4} \left(\frac{\Lambda_{\delta 2}}{m} \right)^2 \right] \frac{e^{-\Lambda_{\delta 2} r_{db}}}{\Lambda_{\delta 2} r_{db}} \right\} (\tau_d \cdot \tau_b)
\end{aligned} \tag{9}$$

$$\begin{aligned}
V_v(r_{db})_F = & \frac{g_{\omega qq}^2}{4\pi} \left\{ \left(\frac{e^{-m_\omega r_{db}}}{r_{db}} \right) - F_{\omega 2} \left(\frac{e^{-\Lambda_{\omega 1} r_{db}}}{r_{db}} \right) + F_{\omega 1} \left(\frac{e^{-\Lambda_{\omega 2} r_{db}}}{r_{db}} \right) \right\} + \frac{1}{6} \frac{g_{\rho qq}^2}{4\pi} \frac{1}{m^2} \left\{ \left(\frac{e^{-m_\rho r_{db}}}{r_{db}} \right) - \right. \\
& \left. F_{\rho 2} \left(\frac{e^{-\Lambda_{\rho 1} r_{db}}}{r_{db}} \right) + F_{\rho 1} \left(\frac{e^{-\Lambda_{\rho 2} r_{db}}}{r_{db}} \right) \right\} (\tau_d \cdot \tau_b) (\sigma_d \cdot \sigma_b)
\end{aligned} \tag{10}$$

The net s-wave OBE potential with finite size effect can be expressed as

$$V_{OBE} = V_{ps}(r_{db})_F + V_s(r_{db})_F + V_v(r_{db})_F \tag{11}$$

$$\begin{aligned}
V_{OBE}(r_{db})_F = & \frac{1}{12} \left[\frac{g_{\pi qq}^2}{4\pi} \left\{ \left(\frac{m_\pi}{m} \right)^2 \frac{e^{-m_\pi r_{db}}}{r_{db}} - (F_{\pi 2}) \left(\frac{\Lambda_{\pi 1}}{m} \right)^2 \frac{e^{-\Lambda_{\pi 1} r_{db}}}{r_{db}} + (F_{\pi 1}) \left(\frac{\Lambda_{\pi 2}}{m} \right)^2 \right. \right. \\
& \left. \left. \frac{e^{-\Lambda_{\pi 2} r_{db}}}{r_{db}} \right\} (\tau_d \cdot \tau_b) + \frac{g_{\eta qq}^2}{4\pi} \left\{ \left(\frac{m_\eta}{m} \right)^2 \frac{e^{-m_\eta r_{db}}}{r_{db}} - (F_{\eta 2}) \left(\frac{\Lambda_{\eta 1}}{m} \right)^2 \frac{e^{-\Lambda_{\eta 1} r_{db}}}{r_{db}} + (F_{\eta 1}) \left(\frac{\Lambda_{\eta 2}}{m} \right)^2 \right. \right. \\
& \left. \left. \frac{e^{-\Lambda_{\eta 2} r_{db}}}{r_{db}} \right\} (\sigma_d \cdot \sigma_b) - \frac{g_{\sigma qq}^2}{4\pi} \left\{ m_\sigma \left[1 - \frac{1}{4} \left(\frac{m_\sigma}{m} \right)^2 \right] \frac{e^{-m_\sigma r_{db}}}{m_\sigma r_{db}} - F_{\sigma 2} \Lambda_{\sigma 1} \left[1 - \frac{1}{4} \left(\frac{\Lambda_{\sigma 1}}{m} \right)^2 \right] \right. \right. \\
& \left. \left. \frac{e^{-\Lambda_{\sigma 1} r_{db}}}{\Lambda_{\sigma 1} r_{db}} + F_{\sigma 1} \Lambda_{\sigma 2} \left[1 - \frac{1}{4} \left(\frac{\Lambda_{\sigma 2}}{m} \right)^2 \right] \frac{e^{-\Lambda_{\sigma 2} r_{db}}}{\Lambda_{\sigma 2} r_{db}} \right\} + \frac{g_{\delta qq}^2}{4\pi} \left\{ m_\delta \left[1 - \frac{1}{4} \left(\frac{m_\delta}{m} \right)^2 \right] \frac{e^{-m_\delta r_{db}}}{m_\delta r_{db}} \right. \right. \\
& \left. \left. - F_{\delta 2} \Lambda_{\delta 1} \left[1 - \frac{1}{4} \left(\frac{\Lambda_{\delta 1}}{m} \right)^2 \right] \frac{e^{-\Lambda_{\delta 1} r_{db}}}{\Lambda_{\delta 1} r_{db}} + F_{\delta 1} \Lambda_{\delta 2} \left[1 - \frac{1}{4} \left(\frac{\Lambda_{\delta 2}}{m} \right)^2 \right] \frac{e^{-\Lambda_{\delta 2} r_{db}}}{\Lambda_{\delta 2} r_{db}} \right\} (\tau_d \cdot \tau_b) + \right. \\
& \left. \frac{g_{\omega qq}^2}{4\pi} \left\{ \left(\frac{e^{-m_\omega r_{db}}}{r_{db}} \right) - F_{\omega 2} \left(\frac{e^{-\Lambda_{\omega 1} r_{db}}}{r_{db}} \right) + F_{\omega 1} \left(\frac{e^{-\Lambda_{\omega 2} r_{db}}}{r_{db}} \right) \right\} + \frac{1}{6} \frac{g_{\rho qq}^2}{4\pi} \frac{1}{m^2} \left\{ \left(\frac{e^{-m_\rho r_{db}}}{r_{db}} \right) \right. \right. \\
& \left. \left. - F_{\rho 2} \left(\frac{e^{-\Lambda_{\rho 1} r_{db}}}{r_{db}} \right) + F_{\rho 1} \left(\frac{e^{-\Lambda_{\rho 2} r_{db}}}{r_{db}} \right) \right\} (\tau_d \cdot \tau_b) (\sigma_d \cdot \sigma_b)
\end{aligned} \tag{12}$$

The overall contribution from OBE is very less due to its delicate cancellation with each other. However, two points should be noted on the overall contribution (attraction/repulsion) of the OBE potential: (i) its contribution is strongly related to the coupling constant of the each individual meson exchange and (ii) it depends on the spin-isospin channels.

The parameters of the model are as follows: (i) hadron masses (ii) coupling constant of the exchange mesons (iii) regularization parameter Λ_α (iv) residual running coupling constant k_{mol} (v) color screening parameter c .

The masses of the hadrons and exchange mesons are taken from the PDG [47]. The coupling constant of the exchange mesons and regularization parameter Λ_α are obtained from refs.[38, 46, 48, 49], also tabulated in Table-I. The estimates of the coupling constants of OBE potential are given in the most of the realistic potentials

[38, 46, 48, 49] which were developed to reproduce NN-phase shift data and to explain the deuteron properties. Hence, we have taken them same as estimated in Refs. [38, 46] and approximated the meson-hadron coupling constant for other hadronic molecular cases as

$$g_{\alpha hh} \simeq g_{\alpha NN} \tag{13}$$

where $g_{\alpha hh}$ and $g_{\alpha NN}$ are the meson-hadron and meson-nucleon coupling constants, respectively. Thus, the masses, exchange meson coupling constant and Λ_α are the fixed parameters and obtained from Refs. [38, 46, 47], also tabulated in Table-?? & I. Apart from these, the residual running coupling constant k_{mol} is calculated by using Eq.(4), and calculated values for attempted di-hadronic systems are tabulated in Table-II. The color screening parameter 'c' is the only free parameter of the

TABLE I: OBE potential parameters, this parameters are taken from [38, 46]

Mesons	π	η	σ	$a_0(\delta)$	ω	ρ
$\frac{g_{\alpha NN}^2}{4\pi}$	13.6	3	7.7823 *	2.6713	20	0.85
Λ_α	1.3	1.5	2.0	2.0	1.5	1.3
Mass (in MeV)	134.9	548.8	710	983	782.6	775.4

(*The $\frac{g_{\alpha NN}^2}{4\pi}$ for the σ -exchange given in the table is used for total isospin $I_T=1$. Whereas for $I_T=0$, $\frac{g_{\alpha NN}^2}{4\pi}=16.2061$ have been used.)

TABLE II: The threshold mass, reduced mass and residual running coupling constant(k_{mol}) of the di-hadronic systems. In the calculation of the k_{mol} the $\Lambda_Q=0.150$ GeV is taken while $n_f=2,3,4$ is taken as per involvement of the light quarks, charm quark and bottom quark, respectively. Here, Σ^* and Ξ^* are $J^P = \frac{3}{2}^+$ constituents.

System	Threshold mass GeV	Reduce mass GeV	k_{mol}	System	Threshold mass GeV	Reduce mass GeV	k_{mol}
$\Sigma_s K^*$	2.088	0.511	0.2882	$\Xi_s K^*$	2.210	0.532	0.2855
$\Sigma_s^* K^*$	2.278	0.543	0.2841	$\Xi_s^* K^*$	2.427	0.565	0.2815
$\Sigma_c K^*$	3.349	0.656	0.2911	$\Xi_c K^*$	3.366	0.657	0.2909
$\Sigma_c^* K^*$	3.414	0.660	0.2906	$\Xi_c^* K^*$	3.541	0.669	0.2896
$\Sigma_b K^*$	6.708	0.776	0.3003	$\Xi_b K^*$	6.683	0.775	0.3003
$\Sigma_b^* K^*$	6.728	0.776	0.3002				
$\Sigma_s D^*$	3.199	0.748	0.2809	$\Xi_s D^*$	3.321	0.794	0.2762
$\Sigma_s^* D^*$	3.389	0.818	0.2739	$\Xi_s^* D^*$	3.538	0.868	0.2692
$\Sigma_c D^*$	4.460	1.103	0.2509	$\Xi_c D^*$	4.477	1.107	0.2506
$\Sigma_c^* D^*$	4.460	1.103	0.2509	$\Xi_c^* D^*$	4.652	1.141	0.2484
$\Sigma_b D^*$	7.819	1.491	0.2477	$\Xi_b D^*$	7.794	1.49	0.2478
$\Sigma_b^* D^*$	7.839	1.493	0.2476				
$\Sigma_s B^*$	6.517	0.974	0.2812	$\Xi_s B^*$	6.64	1.054	0.2747
$\Sigma_s^* B^*$	6.708	1.097	0.2714	$\Xi_s^* B^*$	6.857	1.189	0.2649
$\Sigma_c B^*$	7.778	1.679	0.2392	$\Xi_c B^*$	7.796	1.687	0.2389
$\Sigma_c^* B^*$	7.844	1.709	0.2380	$\Xi_c^* B^*$	7.971	1.767	0.2357
$\Sigma_b B^*$	11.138	2.779	0.2078	$\Xi_b B^*$	11.113	2.773	0.2079
$\Sigma_b^* B^*$	11.157	2.783	0.2077				

model and we fitted it to get the empirical value of binding energy of the deuteron. For $c=0.0686$ GeV, we obtained the binding energy of the deuteron. Hence, we took it as a constant and have not changed for any further calculations of the di-hadronic molecules.

In Fig-1 the characteristic nature of the one meson exchange of OBE potential and in Fig-3 net OBE, Yukawa screen like and effective potential are shown. We can see from the Fig-1(a) & (b) that the all individual meson exchange diminish exponentially at large distance, in which the pion exchange which is being the lightest me-

TABLE III: Mass spectra of proton-neutron (deuteron) and neutron-neutron bound system.

$[I_1(J_1^{P_1})]^{Q_1} - [I_2(J_2^{P_2})]^{Q_2}$	System $I(J^P)$	μ GeV	B.E. MeV	Mass MeV	$\sqrt{r^2}$ fm
$[\frac{1}{2}(\frac{1}{2}^+)]^+ - [\frac{1}{2}(\frac{1}{2}^+)]^0$	$p-n$ $0(1^+)$	0.1090	-2.2211	1.875	03.13
$[\frac{1}{2}(\frac{1}{2}^+)]^0 - [\frac{1}{2}(\frac{1}{2}^+)]^0$	$n-n$ $1(0^+)$	0.1004	+0.9528	1.880	03.40

FIG. 1: The characteristic nature of the s-wave one meson exchange potential (a) in case of proton-neutron (deuteron) system (b) in case of neutron-neutron system

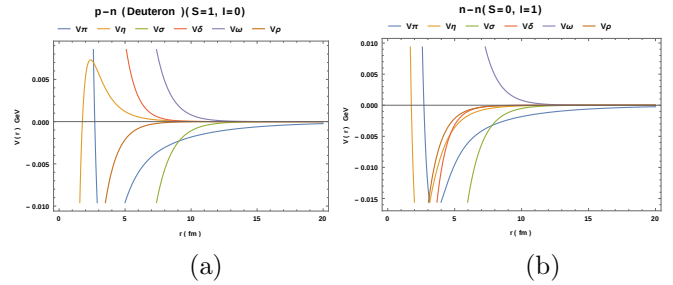


FIG. 2: The characteristic nature of the net s-wave One Boson Exchange (OBE) potential (a) in case of p-n (deuteron) system (b) in case of neutron-neutron system

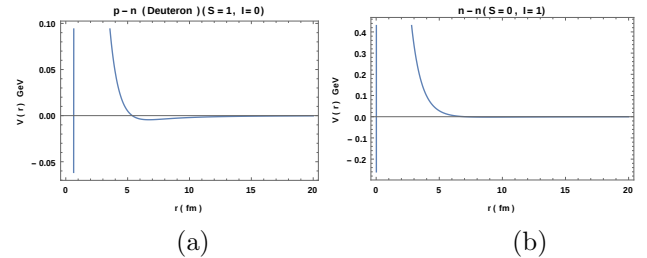
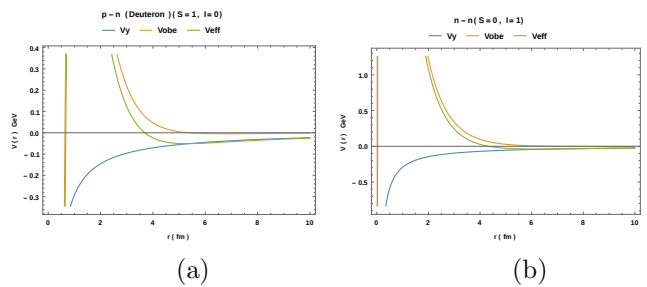


FIG. 3: The characteristic nature of the s-wave OBE potential, screen Yukawa-like potential and net effective potential (a) in case of p-n (deuteron) system (b) in case of neutron-neutron system



son exchange in OBE, contribute up to far distance while the sigma exchange contribute up to mid-range and other

FIG. 4: The characteristic nature of the s-wave OBE potential for the case of $\Sigma_c D^*$ and $\Sigma_c^* D^*$, for all possible spin-isospin channels

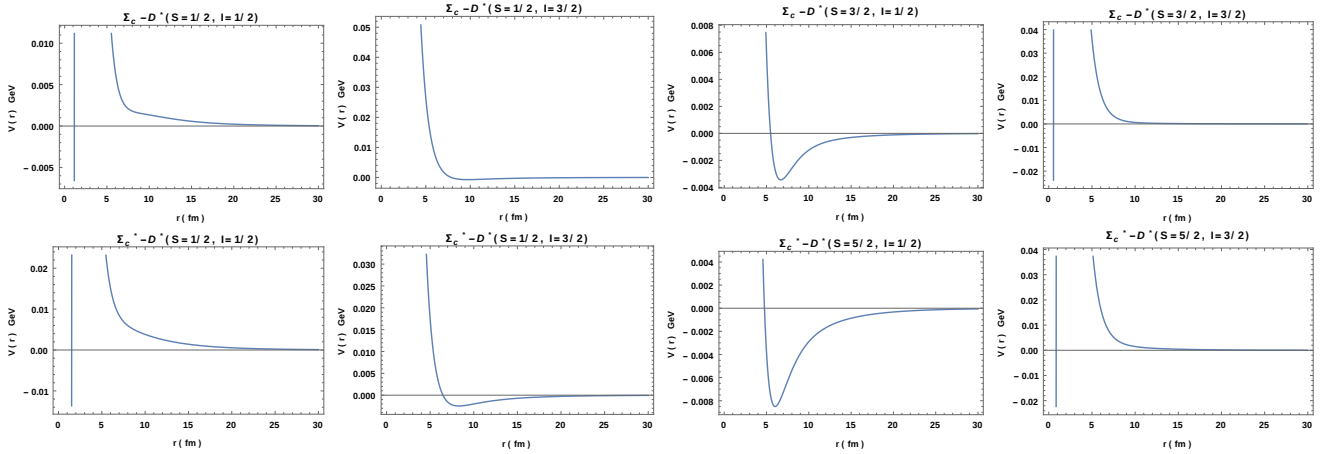
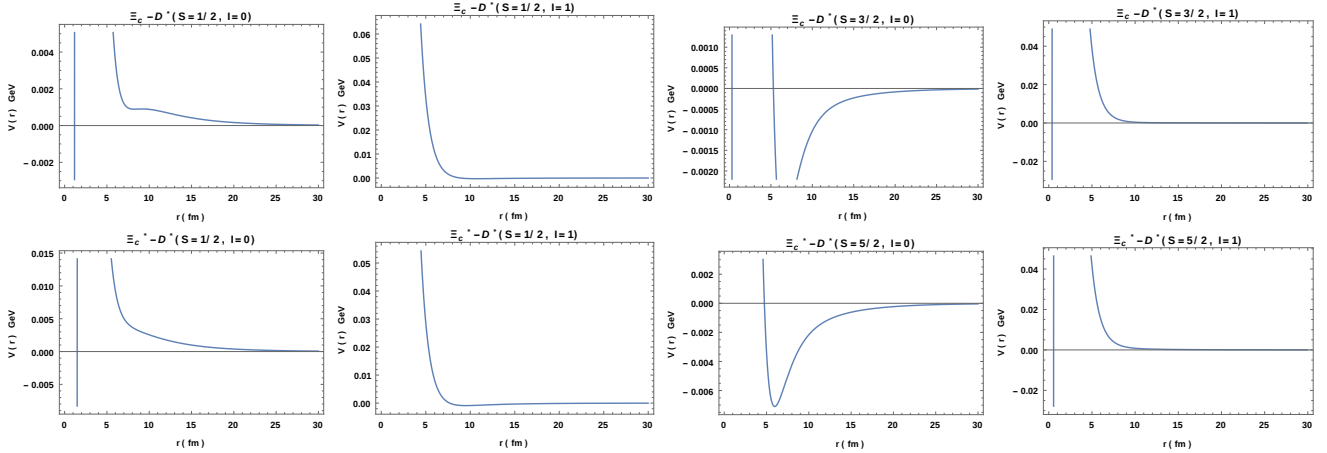


FIG. 5: The characteristic nature of the s-wave OBE potential for the case of $\Xi_c D^*$ and $\Xi_c^* D^*$, for all possible spin-isospin channels



meson effectively contribute at short range. In the case of deuteron, from Fig-1(a), we can see that the pion, sigma and rho meson exchanges are attractive while eta, a_0 (or δ) and omega exchanges are repulsive. The net effective contribution of the s-wave OBE potential is shown in Fig-2. From Fig-2, we can see that in the case of p-n bound state the net effective s-wave OBE potential is very shallow attractive near 3 fm to 6 fm while the potential is repulsive in case of neutron-neutron system. The overall contributory nature of s-wave OBE potential along with screen Yukawa-like and net effective potential can be seen in the Fig-3(a) (b). Fig-3(a) shows very shallow attractive strength at large distance while the net effective potential shows attractive strength near 4 fm due to influence of the attractive Yukawa-like screen potential. Similarly, Fig-1(b) shows the meson exchange behavior in the case of the n-n system. In general, the attractive and repulsiveness of the s-wave one meson exchange potentials are depends on their isospin-spin channels. We can see from Fig-3(b) that the net OBE potential is re-

pulsive at short distance and exponentially diminish at long range. Even, under the influence of the attractive Yukawa-like potential, the net effective potential get almost zero strength or just above the zero, while it is repulsive at short range. As a result, the Fig-3(b) shows that the resultant potential leads n-n systems unbound.

In the Table-III, the binding energy of the pn (deuteron) and nn bound states are tabulated by using $c=0.0686$ GeV with other fixed parameters which are already discussed in above section. The calculated binding energy is in agreement with experimental value 2.224 MeV whereas the obtained mean square root radius is nearly about 3 fm while the expected is near 2.1 fm.

III. MASS SPECTRA OF MESON-BARYON SYSTEMS

We have calculated the mass spectra of the $\Sigma_{s,c,b} K^*$, $\Sigma_{s,c,b} D^*$, $\Sigma_{s,c,b} B^*$, $\Xi_{s,c,b} K^*$, $\Xi_{s,c,b} D^*$ and $\Xi_{s,c,b} B^*$ sys-

tems. The graphs of potential strength verse range for individual meson exchange, net OBE potential, screen Yukawa-like potential and net effective potential are plotted, and are shown in Fig-4 to 7. To understand the behavior of the potentials incorporated in this work with different spin-isospin channels for attempted di-hadronic systems, we present the analysis graphs for one example systems ($\Sigma_c D^*$ and $\Sigma_c^* D^*$). The plots for individual meson exchange and comparative plots of net s-wave OBE, Yukawa-like potential and net effective potentials are shown in Fig- 6 and 7, and presented in appendix.

Fig-4 shows the contributory nature of the effective s-wave OBE potential in all possible spin-isospin channels for $\Sigma_c D^*$ and $\Sigma_c^* D^*$ systems, while Fig-5 present the $\Xi_c D^*$ and $\Xi_c^* D^*$ systems. We can see from the Fig-4, the spin-isospin channel (S,I) = (5/2, 1/2), (3/2, 1/2) and (1/2, 3/2) gets attractive strength near 4-6 fm. Among these three channels, the channel (S,I) = (5/2, 1/2) seems strongest attractive channel. Whereas, the Fig-5 shows that the spin-isospin channel (S,I) = (3/2, 0) and (5/2, 0) channels are attractive. Indeed, with s-wave OBE interaction, all these attractive channels provides the probabilities to get bound states with these specific spin-isospin combination, provided that these attractive strength should strong enough to overcome kinetic energy repulsion. In the present study, to get bound state of the proton-neutron (deuteron) system, the s-wave OBE potential do not get sufficient attractive strength, hence, we need some additional attractive strength to get bound state. Thus, we have incorporated screen Yukawa-like potential along with s-wave OBE potential. All the potential parameters are tuned for deuteron experimental value of binding energy and taken same for all other calculations. The interesting graphs of one meson exchange potential and comparative plots of screen Yukawa-like potential, net s-wave OBE potential and total effective potential are presented in the appendix.

$$\Sigma_{s,c,b} - K^*, \Sigma_{s,c,b} - D^* \text{ and } \Sigma_{s,c,b} - B^* :-$$

The bound states of the di-hadronic systems with a baryon Σ and a mesons K^* , D^* and B^* are calculated, and the results are tabulated in the Table-IV, V and VI. The strength and contribution of the s-wave OBE potential is the delicate cancellation of the individual meson exchange, hence, the Yukawa-like screen potential shows large impact on the net effective interaction potential, where this potential is sensitive to the parameter c (which is fixed at c=0.0686 GeV) and the value of residual coupling constant k_{mol} (which is tabulated in Table-II). Thus, the results are found sensitive to the Yukawa-like screen potential.

The bound states of $\Sigma_{s,c,b} - K^*$ are found in (I,S) = (1/2, 3/2), (1/2, 5/2) and (3/2, 1/2) channels. In the relatively heavier system $\Sigma_{c,b} - K^*$, the channels (3/2, 3/2) and (3/2, 5/2) are also found bound, even, in the $\Sigma_b - K^*$ system the channel (1/2, 1/2) is obtained bound

TABLE IV: Mass spectra of meson-baryon ($\Sigma_{s,c,b} - K^*$) (molecular pentaquark) molecules. Masses of the meson and baryon are taken from PDG [47] which are also listed in Table-???. Here, μ is variational parameter. I (isospin), G (G-parity), J (total angular momentum), Q (charge) and P (parity) are quantum numbers of the respective meson and baryon.

$[I_1(J_1^{P_1})]^{Q_1} - [I_2(J_2^{P_2})]^{Q_2}$	System	$I(J^P)$	μ GeV	B.E. MeV	Mass MeV	$\sqrt{r^2}$ fm
$[1(\frac{1}{2}^+)]^0 - [\frac{1}{2}(1^-)]^0$	$\Sigma_s - K^*$	$\frac{1}{2}(\frac{1}{2}^-)$	0.0071	+0.0038	2.088	47.48
		$\frac{3}{2}(\frac{1}{2}^-)$	0.0572	-0.3704	2.088	05.97
		$\frac{3}{2}(\frac{3}{2}^-)$	0.0767	-0.9909	2.087	04.45
		$\frac{5}{2}(\frac{3}{2}^-)$	0.1077	-1.5888	2.086	03.17
$[1(\frac{3}{2}^+)]^0 - [\frac{1}{2}(1^-)]^0$	$\Sigma_s - K^*$	$\frac{1}{2}(\frac{1}{2}^-)$	0.0066	+0.0029	2.278	52.01
		$\frac{3}{2}(\frac{1}{2}^-)$	0.0466	-0.2289	2.278	07.33
		$\frac{3}{2}(\frac{3}{2}^-)$	0.0555	-0.4650	2.278	06.16
		$\frac{5}{2}(\frac{3}{2}^-)$	0.0072	+0.0033	2.278	47.47
$[1(\frac{1}{2}^+)]^0 - [\frac{1}{2}(1^-)]^0$	$\Sigma_c - K^*$	$\frac{1}{2}(\frac{1}{2}^-)$	0.0039	+0.0007	3.349	86.62
		$\frac{3}{2}(\frac{1}{2}^-)$	0.0781	-1.0945	3.348	04.37
		$\frac{3}{2}(\frac{3}{2}^-)$	0.1059	-2.5205	3.347	03.22
		$\frac{5}{2}(\frac{3}{2}^-)$	0.1003	-1.8426	3.347	03.40
$[1(\frac{3}{2}^+)]^0 - [\frac{1}{2}(1^-)]^0$	$\Sigma_c - K^*$	$\frac{1}{2}(\frac{1}{2}^-)$	0.0039	+0.0007	3.414	85.76
		$\frac{3}{2}(\frac{1}{2}^-)$	0.0666	-0.7637	3.413	05.13
		$\frac{3}{2}(\frac{3}{2}^-)$	0.0819	-1.4690	3.412	04.17
		$\frac{5}{2}(\frac{3}{2}^-)$	0.1349	-3.0589	3.411	02.53
$[1(\frac{1}{2}^+)]^0 - [\frac{1}{2}(1^-)]^0$	$\Sigma_b - K^*$	$\frac{1}{2}(\frac{1}{2}^-)$	0.1666	-6.2422	6.702	02.05
		$\frac{3}{2}(\frac{1}{2}^-)$	0.0939	-1.8751	6.707	03.64
		$\frac{3}{2}(\frac{3}{2}^-)$	0.1309	-4.2306	6.704	02.61
		$\frac{5}{2}(\frac{3}{2}^-)$	0.1003	-2.1359	6.706	03.40
$[1(\frac{3}{2}^+)]^0 - [\frac{1}{2}(1^-)]^0$	$\Sigma_b - K^*$	$\frac{1}{2}(\frac{1}{2}^-)$	0.0026	+0.0002	6.727	130.6
		$\frac{3}{2}(\frac{1}{2}^-)$	0.0886	-1.6678	6.726	03.85
		$\frac{3}{2}(\frac{3}{2}^-)$	0.1176	-3.4806	6.724	02.90
		$\frac{5}{2}(\frac{3}{2}^-)$	0.1054	-2.3474	6.725	03.24

state. The binding energy are appeared in the range from 0.2 MeV to 6 MeV. In the $\Sigma_{s,c} - D^*$ systems all isospin-spin channels are emerged as bound state except (I,S)=(1/2, 1/2) channel, whereas in the $\Sigma_b - D^*$ systems all channel are found bound. In the case of the $\Sigma_{s,c,b} - D^*$ systems, the binding energy are appeared around 0.7 MeV to 7 MeV. On the other hand, the relatively heavier systems $\Sigma_{s,c,b} - B^*$, all isospin-spin channels are appeared as a bound state and the binding energy are found nearly about 0.8 MeV to 7 MeV.

The meson-baryon molecular systems have also been studied by others [22–26, 50]. In Ref. [22], authors were predicted the bound states of molecular pentaquark within one pion exchange framework for possible (I, J^P) combination. For set of values of regularization parameter, they were found binding energy between 1 MeV to 9 MeV. Our results are in agreement with results of Ref. [22]. In Ref.[23], within one boson exchange scheme, the strange hidden-charm pentaquarks was in-

TABLE V: Mass spectra of meson-baryon (molecular pentaquark) ($\Sigma_{s,c,b} - D^*$) molecules. Masses of the meson and baryon are taken from PDG [47] which are also listed in Table-??. Here, μ is variational parameter. I (isospin), G (G-parity), J (total angular momentum), Q (charge) and P (parity) are quantum numbers of the respective meson and baryon.

$[I_1(J_1^{P_1})]^{Q_1} - [I_2(J_2^{P_2})]^{Q_2}$	System	$I(J^P)$	μ GeV	B.E. MeV	Mass GeV	$\sqrt{r^2}$ fm
$[1(\frac{1}{2}^+)]^0 - [\frac{1}{2}(1^-)]^0$	$\Sigma_s - D^*$	$\frac{1}{2}(\frac{1}{2}^-)$	0.0031	+0.0003	3.1996	110.1
		$\frac{1}{2}(\frac{1}{2}^-)$	0.0779	-1.1139	3.198	04.38
		$\frac{1}{2}(\frac{1}{2}^-)$	0.1059	-2.5417	3.197	03.22
		$\frac{1}{2}(\frac{1}{2}^-)$	0.1034	-1.9756	3.197	03.30
$[1(\frac{3}{2}^+)]^0 - [\frac{1}{2}(1^-)]^0$	$\Sigma_s - D^*$	$\frac{1}{2}(\frac{1}{2}^-)$	0.0027	+0.0002	3.389	126.2
		$\frac{1}{2}(\frac{1}{2}^-)$	0.0669	-0.7939	3.388	05.11
		$\frac{1}{2}(\frac{1}{2}^-)$	0.0823	-1.5068	3.388	04.15
		$\frac{1}{2}(\frac{1}{2}^-)$	0.1434	-3.3415	3.386	02.38
$[1(\frac{1}{2}^+)]^0 - [\frac{1}{2}(1^-)]^0$	$\Sigma_c - D^*$	$\frac{1}{2}(\frac{1}{2}^-)$	0.0015	+0.0000	4.460	221.1
		$\frac{1}{2}(\frac{1}{2}^-)$	0.0816	-1.1805	4.459	04.18
		$\frac{1}{2}(\frac{1}{2}^-)$	0.1149	-2.8497	4.457	02.97
		$\frac{1}{2}(\frac{1}{2}^-)$	0.0948	-1.5949	4.459	03.60
$[1(\frac{3}{2}^+)]^0 - [\frac{1}{2}(1^-)]^0$	$\Sigma_c - D^*$	$\frac{1}{2}(\frac{1}{2}^-)$	0.0015	+0.0000	4.525	221.4
		$\frac{1}{2}(\frac{1}{2}^-)$	0.0729	-0.9285	4.524	04.68
		$\frac{1}{2}(\frac{1}{2}^-)$	0.0945	-1.9401	4.523	03.61
		$\frac{1}{2}(\frac{1}{2}^-)$	0.1078	-2.0183	4.523	03.16
$[1(\frac{1}{2}^+)]^0 - [\frac{1}{2}(1^-)]^0$	$\Sigma_b - D^*$	$\frac{1}{2}(\frac{1}{2}^-)$	0.1530	-4.7770	7.8152	02.23
		$\frac{1}{2}(\frac{1}{2}^-)$	0.1044	-1.2479	7.8187	03.27
		$\frac{1}{2}(\frac{1}{2}^-)$	0.1275	-3.5372	7.8164	02.68
		$\frac{1}{2}(\frac{1}{2}^-)$	0.0928	-1.5886	7.8183	03.68
$[1(\frac{3}{2}^+)]^0 - [\frac{1}{2}(1^-)]^0$	$\Sigma_b - D^*$	$\frac{1}{2}(\frac{1}{2}^-)$	0.2285	-7.7376	7.831	01.49
		$\frac{1}{2}(\frac{1}{2}^-)$	0.0844	-1.3127	7.837	04.05
		$\frac{1}{2}(\frac{1}{2}^-)$	0.1167	-3.0135	7.836	02.92
		$\frac{1}{2}(\frac{1}{2}^-)$	0.0963	-1.7036	7.837	03.54

investigated and the binding energy of bound states were predicted about 0.5 MeV to 15 MeV. Jia-Jun Wu et. al. [50] predicted relatively narrow and dynamically generated meson-baryon resonance near 4.3 GeV within the coupled-channel unitary approach with the local hidden gauge formalism. Jia-Jun Wu et. al. [50] studied the coupled channel interaction of $\overline{D}\Sigma_c - \overline{D}\Lambda_c$, $\overline{D}^*\Sigma_c - \overline{D}^*\Lambda_c$ channels. We have not attempted the channel coupling in the present study. However, we obtained bound states near 4.46 GeV and 4.52 GeV in $\Sigma_c D^*$ and $\Sigma_c^* D^*$ system, respectively. Whereas, the bound states are appeared near 4.47 GeV and 4.66 GeV in $\Xi_c D^*$ and $\Xi_c^* D^*$. Aziz et. al. [25] studied $P_c(4380)$ and $P_c(4450)$ states as pentaquark states in the molecular picture with QCD sum rules, moreover, they have predicted hidden bottom pentaquark states in [24] as possible partner of these states. These two new states as $P_c(4380)$ and $P_c(4450)$ with the preferred J^P assignments are of opposite parity, with one state having spin $\frac{3}{2}$ and the other $\frac{5}{2}$, were reported

TABLE VI: Mass spectra of meson-baryon (molecular pentaquark) ($\Sigma_{s,c,b} - B^*$) molecules. Masses of the meson and baryon are taken from PDG [47] which are also listed in Table-??. Here, μ is variational parameter. I (isospin), G (G-parity), J (total angular momentum), Q (charge) and P (parity) are quantum numbers of the respective meson and baryon.

$[I_1(J_1^{P_1})]^{Q_1} - [I_2(J_2^{P_2})]^{Q_2}$	System	$I(J^P)$	μ GeV	B.E. MeV	Mass MeV	$\sqrt{r^2}$ fm
$[1(\frac{1}{2}^+)]^0 - [\frac{1}{2}(1^-)]^0$	$\Sigma_s - B^*$	$\frac{1}{2}(\frac{1}{2}^-)$	0.1717	-6.3149	6.511	01.99
		$\frac{1}{2}(\frac{1}{2}^-)$	0.0927	-1.7796	6.516	03.68
		$\frac{1}{2}(\frac{1}{2}^-)$	0.1306	-4.0935	6.513	02.61
		$\frac{1}{2}(\frac{1}{2}^-)$	0.0996	-2.0467	6.515	03.43
$[1(\frac{3}{2}^+)]^0 - [\frac{1}{2}(1^-)]^0$	$\Sigma_s - B^*$	$\frac{1}{2}(\frac{1}{2}^-)$	0.0014	+0.0000	6.707	242.4
		$\frac{1}{2}(\frac{1}{2}^-)$	0.0871	-1.5525	6.706	03.92
		$\frac{1}{2}(\frac{1}{2}^-)$	0.1169	-3.3143	6.704	02.92
		$\frac{1}{2}(\frac{1}{2}^-)$	0.1043	-2.2036	6.705	03.27
$[1(\frac{1}{2}^+)]^0 - [\frac{1}{2}(1^-)]^0$	$\Sigma_c - B^*$	$\frac{1}{2}(\frac{1}{2}^-)$	0.1507	-4.4956	7.774	02.26
		$\frac{1}{2}(\frac{1}{2}^-)$	0.0863	-1.3202	7.777	03.96
		$\frac{1}{2}(\frac{1}{2}^-)$	0.1253	-3.3102	7.775	02.72
		$\frac{1}{2}(\frac{1}{2}^-)$	0.0908	-1.4599	7.777	03.76
$[1(\frac{3}{2}^+)]^0 - [\frac{1}{2}(1^-)]^0$	$\Sigma_c - B^*$	$\frac{1}{2}(\frac{1}{2}^-)$	0.2219	-7.1896	7.8368	01.53
		$\frac{1}{2}(\frac{1}{2}^-)$	0.0822	-1.1899	7.842	04.15
		$\frac{1}{2}(\frac{1}{2}^-)$	0.1144	-2.7919	7.841	02.98
		$\frac{1}{2}(\frac{1}{2}^-)$	0.0938	-1.5453	7.842	03.64
$[1(\frac{1}{2}^+)]^0 - [\frac{1}{2}(1^-)]^0$	$\Sigma_b - B^*$	$\frac{1}{2}(\frac{1}{2}^-)$	0.1279	-2.9231	11.135	02.67
		$\frac{1}{2}(\frac{1}{2}^-)$	0.0786	-0.9082	11.137	04.34
		$\frac{1}{2}(\frac{1}{2}^-)$	0.1177	-2.5259	11.135	02.90
		$\frac{1}{2}(\frac{1}{2}^-)$	0.0805	-0.9545	11.137	04.24
$[1(\frac{3}{2}^+)]^0 - [\frac{1}{2}(1^-)]^0$	$\Sigma_b - B^*$	$\frac{1}{2}(\frac{1}{2}^-)$	0.1418	-3.4602	11.153	02.41
		$\frac{1}{2}(\frac{1}{2}^-)$	0.0768	-0.8649	11.156	04.45
		$\frac{1}{2}(\frac{1}{2}^-)$	0.1122	-2.3129	11.154	03.04
		$\frac{1}{2}(\frac{1}{2}^-)$	0.0819	-0.9863	11.156	04.17

in 2015 by LHCb-collaboration [2]. In the present formalism $P_c(4450)$ is identified as $\Sigma_c - D^*$ molecular pentaquark with $(I,S)=(\frac{1}{2},\frac{3}{2})$ with negative parity whereas the $P_c(4380)$ is not predicted within present study. The threshold of the $\Sigma_c - D^*$ is 4460.72 MeV, if $P_c(4450)$ with mass 4449.8 ± 1.7 MeV and width $39 \pm 5 \pm 8$ MeV is a $\Sigma_c - D^*$ bound state molecule then it required binding energy approximately 10.92 MeV below the threshold. On the other hand, $P_c(4380)$ is required deep binding of approximately 80 MeV for molecular structure. Hence, $P_c(4450)$ is naturally look like loosely bound molecular candidate while $P_c(4380)$ with deep binding and large width is very unlikely to be molecular nature. The present formalism predict $P_c(4450)$ as a $\Sigma_c - D^*$ bound state with $I(J^P) = \frac{1}{2}(\frac{3}{2}^-)$.

TABLE VII: Mass spectra of meson-baryon (molecular pentaquark) $\Xi_{s,c,b} - K^*$ molecules. Masses of the meson and baryon are taken from PDG [47] which are also listed in Table-??. Here, μ is variational parameter. I (isospin), G (G-parity), J (total angular momentum), Q (charge) and P (parity) are quantum numbers of the respective meson and baryon.

$[I_1(J_1^{P_1})]^{Q_1} - [I_2(J_2^{P_2})]^{Q_2}$	System	$I(J^P)$	μ GeV	B.E. MeV	Mass MeV	$\sqrt{r^2}$ fm
$[\frac{1}{2}(\frac{1}{2}^+)]^0 - [\frac{1}{2}(1^-)]^0$	$\Xi_s - K^*$	$0(\frac{1}{2}^-)$	0.0063	+0.0027	2.210	54.54
		$1(\frac{3}{2}^-)$	0.0596	-0.3899	2.210	05.73
		$0(\frac{3}{2}^-)$	0.0994	-1.9759	2.208	03.43
		$1(\frac{5}{2}^-)$	0.0764	-0.7226	2.210	04.47
$[\frac{1}{2}(\frac{3}{2}^+)]^0 - [\frac{1}{2}(1^-)]^0$	$\Xi_s - K^*$	$0(\frac{1}{2}^-)$	0.0057	+0.0019	2.427	59.95
		$1(\frac{3}{2}^-)$	0.0535	-0.3139	2.427	06.39
		$0(\frac{3}{2}^-)$	0.0732	-1.0271	2.426	04.66
		$1(\frac{5}{2}^-)$	0.0947	-1.2009	2.426	03.60
$[\frac{1}{2}(\frac{1}{2}^+)]^0 - [\frac{1}{2}(1^-)]^0$	$\Xi_c - K^*$	$0(\frac{1}{2}^-)$	0.0038	+0.0006	3.366	90.93
		$1(\frac{3}{2}^-)$	0.0737	-0.8884	3.365	04.63
		$0(\frac{3}{2}^-)$	0.1306	-4.0298	3.362	02.61
		$1(\frac{5}{2}^-)$	0.0824	-1.1341	3.365	04.14
$[\frac{1}{2}(\frac{3}{2}^+)]^0 - [\frac{1}{2}(1^-)]^0$	$\Xi_c - K^*$	$0(\frac{1}{2}^-)$	0.0037	+0.0006	3.550	92.80
		$1(\frac{3}{2}^-)$	0.0683	-0.7507	3.550	05.00
		$0(\frac{3}{2}^-)$	0.1027	-2.5459	3.548	03.32
		$1(\frac{5}{2}^-)$	0.0891	-1.3392	3.549	03.83
$[\frac{1}{2}(\frac{1}{2}^+)]^0 - [\frac{1}{2}(1^-)]^0$	$\Xi_b - K^*$	$0(\frac{1}{2}^-)$	0.2133	-9.5451	6.674	01.60
		$1(\frac{3}{2}^-)$	0.0843	-1.3986	6.682	04.05
		$0(\frac{3}{2}^-)$	0.1608	-6.4365	6.677	02.12
		$1(\frac{5}{2}^-)$	0.0868	-1.4863	6.682	03.93

$\Xi_{s,c,b} - K^*$, $\Xi_{s,c,b} - D^*$ and $\Xi_{s,c,b} - B^*$:-

The bound states of the di-hadronic systems with a Baryon Ξ and a mesons K^* , D^* and B^* are calculated, and the results are tabulated in the Table-VII, VIII and IX. The bound states of $\Xi_{s,c,b} - K^*$ are appeared in (I,S) = (0, 3/2), (0, 5/2), (1, 5/2), (1, 3/2), (1, 1/2) channels. While, the (0, 1/2) channel obtained as a bound state only for $\Xi_b - K^*$ system. The binding energies are appeared around 0.3 MeV to 9 MeV. Similarly, for the $\Xi_{s,c,b} - D^*$ systems, the (0, 1/2) channel is bound in only for $\Xi_b - D^*$ case, whereas all other channels are found bound state in all cases. The binding energy are found about 0.7 MeV to 7 MeV. In the case of relatively heavier system $\Xi_{s,c,b} - B^*$, the (I,S)=(0, 1/2) is unbound for $\Xi_{s,c} - B^*$ systems, whereas, all other isospin-spin channels are found bound states in the $\Xi_{s,c,b} - B^*$ systems. The binding energies are appeared around 0.6 MeV to 9 MeV. Rui-Chen et. al.[23] have investigated strange hidden-charm pentaquarks states within one boson exchange scheme, and predicted $\Xi_c' \bar{D}^*$ state with $I(J^P) = 0(\frac{1}{2}^-)$ and $\Xi_c^* \bar{D}^*$ state with $0(\frac{1}{2}^-)$ and $0(\frac{3}{2}^-)$. They have

TABLE VIII: Mass spectra of meson-baryon (molecular pentaquark) $\Xi_{s,c,b} - D^*$ molecules. Masses of the meson and baryon are taken from PDG [47] which are also listed in Table-??. Here, μ is variational parameter. I (isospin), G (G-parity), J (total angular momentum), Q (charge) and P (parity) are quantum numbers of the respective meson and baryon.

$[I_1(J_1^{P_1})]^{Q_1} - [I_2(J_2^{P_2})]^{Q_2}$	System	$I(J^P)$	μ GeV	B.E. MeV	Mass MeV	$\sqrt{r^2}$ fm
$[\frac{1}{2}(\frac{1}{2}^+)]^0 - [\frac{1}{2}(1^-)]^0$	$\Xi_s - D^*$	$0(\frac{1}{2}^-)$	0.0027	+0.0002	3.321	128.7
		$1(\frac{3}{2}^-)$	0.0744	-0.9313	3.320	04.59
		$0(\frac{3}{2}^-)$	0.1333	-4.1971	3.317	02.56
		$1(\frac{5}{2}^-)$	0.0837	-1.1954	3.320	04.08
$[\frac{1}{2}(\frac{3}{2}^+)]^0 - [\frac{1}{2}(1^-)]^0$	$\Xi_s - D^*$	$0(\frac{1}{2}^-)$	0.0023	+0.0001	3.538	148.4
		$1(\frac{3}{2}^-)$	0.0685	-0.7754	3.537	04.98
		$0(\frac{3}{2}^-)$	0.1038	-2.6032	3.536	03.29
		$1(\frac{5}{2}^-)$	0.0903	-1.3857	3.537	03.78
$[\frac{1}{2}(\frac{1}{2}^+)]^0 - [\frac{1}{2}(1^-)]^0$	$\Xi_c - D^*$	$0(\frac{1}{2}^-)$	0.0015	+0.0000	4.477	232.8
		$1(\frac{3}{2}^-)$	0.0744	-0.8932	4.476	04.59
		$0(\frac{3}{2}^-)$	0.1438	-4.5849	4.473	02.37
		$1(\frac{5}{2}^-)$	0.0795	-1.0254	4.476	04.30
$[\frac{1}{2}(\frac{3}{2}^+)]^0 - [\frac{1}{2}(1^-)]^0$	$\Xi_c - D^*$	$0(\frac{1}{2}^-)$	0.0014	+0.0000	4.661	242.9
		$1(\frac{3}{2}^-)$	0.0703	-0.7859	4.661	04.85
		$0(\frac{3}{2}^-)$	0.1182	-3.2173	4.658	02.89
		$1(\frac{5}{2}^-)$	0.0826	-1.0998	4.660	04.13
$[\frac{1}{2}(\frac{1}{2}^+)]^0 - [\frac{1}{2}(1^-)]^0$	$\Xi_b - D^*$	$0(\frac{1}{2}^-)$	0.1989	-7.6632	7.787	01.71
		$1(\frac{3}{2}^-)$	0.0781	-1.0319	7.793	04.37
		$0(\frac{3}{2}^-)$	0.1599	-5.6126	7.789	02.13
		$1(\frac{5}{2}^-)$	0.0798	-1.0799	7.793	04.28

predicted binding energies in the range from 0.5 to 15 MeV. Our results of binding energies for these isospin-spin channels are in agreement with reported in Ref. [23]. These results are shown very interesting near threshold bound states possibilities.

IV. RESULTS OF a_s AND r_e FROM COMPOSITENESS THEOREM

In the Sixties, Weinberg [51] suggested in a sophisticated way that the deuteron were a composite particle. In his novel work, he tried to show an elegant model-independent way to identify whether a particle is in a bare elementary state or in a composite state. The conclusion was based on a generalization of Levinson's theorem which gives the formulas for scattering length a_s and effective range r_e in terms of Z , where Z is the "field renormalization" constant [51],

$$\begin{aligned} a_s &= [2(1-Z)/(2-Z)]R + \mathcal{O}(1/\beta) \\ r_e &= [-Z/(1-Z)]R + \mathcal{O}(1/\beta) \end{aligned} \quad (14)$$

TABLE IX: Mass spectra of meson-baryon (molecular pentaquark) $\Xi_{s,c,b} - B^*$ molecules. Masses of the meson and baryon are taken from PDG [47] which are also listed in Table-??. Here, μ is variational parameter. I (isospin), G (G-parity), J (total angular momentum), Q (charge) and P (parity) are quantum numbers of the respective meson and baryon.

$[I_1(J_1^{P_1})]^{Q_1} - [I_2(J_2^{P_2})]^{Q_2}$	System	$I(J^P)$	μ GeV	B.E. MeV	Mass MeV	$\sqrt{r^2}$ fm
$[\frac{1}{2}(\frac{1}{2}^+)]^0 - [\frac{1}{2}(1^-)]^0$	$\Xi_s - B^*$	$0(\frac{1}{2}^-)$	0.2238	-9.6429	6.630	01.52
		$1(\frac{3}{2}^-)$	0.0824	-1.2782	6.638	04.14
		$0(\frac{3}{2}^-)$	0.1619	-6.2356	6.633	02.10
		$1(\frac{5}{2}^-)$	0.0849	-1.3602	6.638	04.02
$[\frac{1}{2}(\frac{3}{2}^+)]^0 - [\frac{1}{2}(1^-)]^0$	$\Xi_s - B^*$	$0(\frac{1}{2}^-)$	0.0012	+0.0000	6.857	287.6
		$1(\frac{3}{2}^-)$	0.0789	-1.1323	6.855	04.33
		$0(\frac{3}{2}^-)$	0.1434	-4.9749	6.852	02.38
		$1(\frac{5}{2}^-)$	0.0851	-1.3221	6.855	04.01
$[\frac{1}{2}(\frac{1}{2}^+)]^0 - [\frac{1}{2}(1^-)]^0$	$\Xi_c - B^*$	$0(\frac{1}{2}^-)$	0.1959	-7.2349	7.788	01.74
		$1(\frac{3}{2}^-)$	0.0759	-0.9353	7.795	04.49
		$0(\frac{3}{2}^-)$	0.1574	-5.2851	7.790	02.17
		$1(\frac{5}{2}^-)$	0.0777	-0.9789	7.795	04.39
$[\frac{1}{2}(\frac{3}{2}^+)]^0 - [\frac{1}{2}(1^-)]^0$	$\Xi_c - B^*$	$0(\frac{1}{2}^-)$	0.0006	$+2.3 \times 10^{-6}$	7.980	569.9
		$1(\frac{3}{2}^-)$	0.0738	-0.8626	7.979	04.63
		$0(\frac{3}{2}^-)$	0.1425	-4.4301	7.975	02.39
		$1(\frac{5}{2}^-)$	0.0779	-0.9682	7.979	04.38
$[\frac{1}{2}(\frac{1}{2}^+)]^0 - [\frac{1}{2}(1^-)]^0$	$\Xi_b - B^*$	$0(\frac{1}{2}^-)$	0.1641	-4.8455	11.108	02.08
		$1(\frac{3}{2}^-)$	0.0681	-0.6105	11.112	05.02
		$0(\frac{3}{2}^-)$	0.1492	-4.1776	11.109	02.29
		$1(\frac{5}{2}^-)$	0.0688	-0.6244	11.112	04.96

where R is the size of the molecular or composite state and is determined by $R \equiv \frac{1}{\sqrt{2\mu\epsilon}}$, here, ϵ is the binding energy and μ is the reduced mass of the composite system (note that we chose binding energy ϵ positive for Eq.(14), the bound state is located at $\epsilon = -\epsilon$). The $\mathcal{O}(1/\beta)$ is the range correction and β is the inverse range of the force and could be calculated if one know the information of the interaction and it is expected to be of the order of magnitude of the inverse of the mass of the exchange particle, in some extent, it is expected to be $m_\pi^{-1} \simeq 1.41$ fm. In order to determine the state of the particle as in a bare elementary or in a composite state, Weinberg argued that the renormalization constant Z take the value $0 \leq Z \leq 1$. If Z=0 then the particle is in a pure composite state while for Z=1 it becomes a purely elementary.

for Z=0 (deuteron as a composite particle), Eq(1) becomes $a_s = R$ and $r_e = \mathcal{O}(1/\beta)$ which is in agreement with the experimental vales : $a_s = +5.41$ fm, $r_e = +1.75$ fm. for deuteron binding energy $\epsilon = 2.22457 MeV \Rightarrow \sqrt{2\mu\epsilon} = 45.7 MeV = 0.23 fm^{-1}$. In contrast, if the deuteron has a significant probability Z (> 0.2) of being found in an elementary (confined) state then a_s would be less than R, and r_e would be large and negative which

would be in contradict with experimental values.

The results of the scattering length (a_s) and effective range (r_e) are obtained by using Eq(14).The results of a_s and r_e for meson-baryon systems, by using the calculated binding energy are shown in the Table-X.

The state $P_c(4450)$ for which the calculated binding energy is underestimated about few MeV, while with the expected binding energy (10.92 MeV) the effective range gain negative value from Z=0.6. The expected binding energy is almost close to its natural energy scale which is about 9 MeV if it has $\Sigma_c D^*$ in its substructure. The large scattering length and positive r_e for Z \rightarrow 0 and binding energy near to expected natural energy scale for $P_c(4450)$ are indicating molecular structure of the state.

V. DISCUSSION AND SUMMARY

In this chapter, we have used the s-wave One Boson Exchange (OBE) potential. We have discussed the characteristic contribution of the individual s-wave one meson exchange potential to the net s-wave OBE potential in respective isospin-spin channels. The strength and contribution of the s-wave OBE potential is the delicate cancellation of the individual meson exchange, hence, the Yukawa-like screen potential shows large impact on the net effective interaction potential, where this potential is sensitive to the parameter c (which is fixed at $c=0.0686$ GeV) and the value of residual coupling constant k_{mol} . Thus, the results are found sensitive to the Yukawa-like screen potential. We have proposed this additional Yukawa-like screen potential to get additional attractive strength with approximation that the two hadrons are experienced the dipole-like interaction.

With the effective interaction potential, we are able to calculate the mass spectra of meson-baryon and di-baryon (antibaryon) molecular states. The obtained results have predicted some interesting molecular pentaquark and hexaquark states with open as well as hidden flavour (strange, charm, bottom), such as $\Sigma_{s,c,b} K^*$, $\Sigma_{s,c,b} D^*$, $\Sigma_{s,c,b} B^*$, $\Xi_{s,c,b} K^*$, $\Xi_{s,c,b} D^*$, $\Xi_{s,c,b} B^*$, $\Sigma_{s,c,b} \Sigma_{s,c,b}$, $\Sigma_{s,c,b} \bar{\Sigma}_{s,c,b}$, $\Xi_{s,c,b} \Xi_{s,c,b}$ and $\Xi_{s,c,b} \bar{\Xi}_{s,c,b}$. The calculated results have compared with work of others. We have predicted some interesting near threshold and shallow bound states. The recently observed state $P_c(4450)$ which is supposed to have minimum five quarks in its internal structure is identified as a bound $\Sigma_c D^*$ state with $I(J^P) = \frac{1}{2}(\frac{3}{2}^-)$. This state $P_c(4450)$ together with $P_c(4380)$ were reported by LHCb collaboration in 2015 [2]. The entire mass spectra presented in this paper have provided the possibilities of resonance like structure, either just above the threshold or bound state (just below the threshold) and provides the reference for searches of such molecular structures in future experiments.

TABLE X: The scattering length a_s and effective range r_e are calculated for meson-baryon systems by using Eq.(14) for different values of renormalization constant Z . The range correction $\mathcal{O}(1/\beta)$ is considered as m_π^{-1} . The values of a_s and r_e are in fm. Binding energies are taken from the results of chapter-??

$I(J^P)$	State	Z=0		Z=0.2		Z=0.4		Z=0.5		Z=0.6		Z=0.9		Z=1	
		a_s	r_e	a_s	r_e	a_s	r_e	a_s	r_e	a_s	r_e	a_s	r_e	a_s	r_e
$\frac{3}{2}(\frac{1}{2}^-)$	$\Sigma_s K^*$	11.6	1.46	10.47	-1.07	9.06	-5.3	8.22	-8.67	7.25	-13.74	3.3	-89.76	1.46	-
$\frac{1}{2}(\frac{1}{2}^-)$	$\Sigma_s K^*$	7.66	1.46	6.97	-0.09	6.11	-2.67	5.59	-4.74	5	-7.83	2.59	-54.31	1.46	-
$\frac{3}{2}(\frac{3}{2}^-)$	$\Sigma_s K^*$	6.36	1.46	5.81	0.24	5.13	-1.8	4.72	-3.43	4.26	-5.88	2.35	-42.59	1.46	-
$\frac{1}{2}(\frac{3}{2}^-)$	$\Sigma_s^* K^*$	10.24	1.46	9.26	-0.73	8.04	-4.39	7.31	-7.31	6.48	-11.7	3.06	-77.52	1.46	-
$\frac{3}{2}(\frac{1}{2}^-)$	$\Sigma_s D^*$	6.3	1.46	5.76	0.25	5.09	-1.76	4.68	-3.37	4.22	-5.79	2.34	-42.04	1.46	-
$\frac{1}{2}(\frac{1}{2}^-)$	$\Sigma_s D^*$	4.66	1.46	4.31	0.66	3.86	-0.67	3.6	-1.74	3.29	-3.34	2.04	-27.34	1.46	-
$\frac{3}{2}(\frac{3}{2}^-)$	$\Sigma_s D^*$	5.09	1.46	4.69	0.55	4.18	-0.96	3.88	-2.17	3.54	-3.98	2.12	-31.2	1.46	-
$\frac{1}{2}(\frac{3}{2}^-)$	$\Sigma_s^* D^*$	5.43	1.46	4.99	0.47	4.44	-1.19	4.11	-2.51	3.73	-4.5	2.18	-34.29	1.46	-
$\frac{3}{2}(\frac{3}{2}^-)$	$\Sigma_s^* D^*$	4.13	1.46	3.83	0.8	3.46	-0.32	3.24	-1.21	2.99	-2.54	1.95	-22.55	1.46	-
$\frac{1}{2}(\frac{1}{2}^-)$	$\Sigma_s B^*$	3.24	1.46	3.04	1.02	2.8	0.28	2.65	-0.32	2.48	-1.21	1.79	-14.55	1.46	-
$\frac{3}{2}(\frac{1}{2}^-)$	$\Sigma_s B^*$	4.81	1.46	4.44	0.62	3.98	-0.77	3.7	-1.89	3.38	-3.56	2.07	-28.7	1.46	-
$\frac{3}{2}(\frac{3}{2}^-)$	$\Sigma_s B^*$	3.67	1.46	3.43	0.91	3.12	-0.01	2.93	-0.75	2.72	-1.85	1.86	-18.42	1.46	-
$\frac{1}{2}(\frac{3}{2}^-)$	$\Sigma_s B^*$	4.59	1.46	4.24	0.68	3.81	-0.62	3.54	-1.66	3.25	-3.22	2.03	-26.66	1.46	-
$\frac{3}{2}(\frac{1}{2}^-)$	$\Sigma_s^* B^*$	3.78	1.46	3.52	0.88	3.2	-0.08	3	-0.85	2.78	-2.01	1.88	-19.36	1.46	-
$\frac{1}{2}(\frac{3}{2}^-)$	$\Sigma_s^* B^*$	4.3	1.46	3.98	0.75	3.59	-0.43	3.35	-1.38	3.08	-2.79	1.98	-24.07	1.46	-
$\frac{3}{2}(\frac{1}{2}^-)$	$\Sigma_c K^*$	6.67	1.46	6.09	0.16	5.37	-2.01	4.93	-3.74	4.44	-6.35	2.41	-45.39	1.46	-
$\frac{1}{2}(\frac{1}{2}^-)$	$\Sigma_c K^*$	4.89	1.46	4.51	0.6	4.03	-0.83	3.75	-1.97	3.42	-3.68	2.09	-29.41	1.46	-
$\frac{3}{2}(\frac{3}{2}^-)$	$\Sigma_c K^*$	5.47	1.46	5.03	0.46	4.47	-1.21	4.14	-2.55	3.75	-4.56	2.19	-34.65	1.46	-
$\frac{1}{2}(\frac{3}{2}^-)$	$\Sigma_c^* K^*$	5.94	1.46	5.44	0.34	4.82	-1.52	4.45	-3.02	4.02	-5.26	2.28	-38.85	1.46	-
$\frac{3}{2}(\frac{3}{2}^-)$	$\Sigma_c^* K^*$	4.57	1.46	4.22	0.69	3.79	-0.61	3.53	-1.64	3.24	-3.19	2.03	-26.47	1.46	-
$\frac{3}{2}(\frac{1}{2}^-)$	$\Sigma_c D^*$	5.33	1.46	4.9	0.5	4.36	-1.11	4.04	-2.4	3.67	-4.34	2.16	-33.32	1.46	-
$\frac{1}{2}(\frac{1}{2}^-)$	$\Sigma_c D^*$	3.95	1.46	3.67	0.84	3.33	-0.2	3.12	-1.03	2.88	-2.27	1.91	-20.93	1.46	-
$\frac{3}{2}(\frac{3}{2}^-)$	$\Sigma_c D^*$	4.79	1.46	4.42	0.63	3.96	-0.75	3.68	-1.86	3.36	-3.53	2.07	-28.46	1.46	-
$\frac{1}{2}(\frac{3}{2}^-)$	$\Sigma_c^* D^*$	4.46	1.46	4.13	0.71	3.71	-0.54	3.46	-1.54	3.17	-3.03	2.01	-25.51	1.46	-
$\frac{3}{2}(\frac{3}{2}^-)$	$\Sigma_c^* D^*$	4.4	1.46	4.07	0.73	3.67	-0.5	3.42	-1.48	3.14	-2.95	2	-24.99	1.46	-
$\frac{1}{2}(\frac{1}{2}^-)$	$\Sigma_c B^*$	3.07	1.46	2.89	1.06	2.67	0.39	2.53	-0.14	2.38	-0.95	1.75	-12.99	1.46	-
$\frac{3}{2}(\frac{1}{2}^-)$	$\Sigma_c B^*$	4.42	1.46	4.1	0.72	3.68	-0.51	3.44	-1.5	3.16	-2.98	2	-25.21	1.46	-
$\frac{1}{2}(\frac{3}{2}^-)$	$\Sigma_c B^*$	3.33	1.46	3.13	0.99	2.87	0.21	2.71	-0.41	2.53	-1.34	1.8	-15.38	1.46	-
$\frac{3}{2}(\frac{3}{2}^-)$	$\Sigma_c B^*$	4.28	1.46	3.97	0.76	3.58	-0.42	3.34	-1.36	3.07	-2.76	1.97	-23.9	1.46	-
$\frac{1}{2}(\frac{3}{2}^-)$	$\Sigma_c^* B^*$	3.48	1.46	3.26	0.96	2.98	0.12	2.81	-0.56	2.62	-1.57	1.83	-16.71	1.46	-
$\frac{3}{2}(\frac{3}{2}^-)$	$\Sigma_c^* B^*$	4.18	1.46	3.87	0.78	3.5	-0.35	3.27	-1.25	3.01	-2.61	1.96	-22.97	1.46	-
$\frac{1}{2}(\frac{1}{2}^-)$	$\Sigma_b K^*$	3.47	1.46	3.24	0.96	2.97	0.13	2.8	-0.54	2.61	-1.54	1.83	-16.58	1.46	-
$\frac{3}{2}(\frac{1}{2}^-)$	$\Sigma_b K^*$	5.12	1.46	4.71	0.55	4.2	-0.98	3.9	-2.2	3.55	-4.02	2.13	-31.45	1.46	-
$\frac{1}{2}(\frac{3}{2}^-)$	$\Sigma_b K^*$	3.9	1.46	3.63	0.85	3.29	-0.16	3.09	-0.97	2.85	-2.19	1.9	-20.45	1.46	-
$\frac{3}{2}(\frac{3}{2}^-)$	$\Sigma_b K^*$	4.89	1.46	4.51	0.61	4.03	-0.82	3.75	-1.96	3.42	-3.68	2.08	-29.38	1.46	-
$\frac{1}{2}(\frac{3}{2}^-)$	$\Sigma_b^* K^*$	4.15	1.46	3.85	0.79	3.47	-0.33	3.25	-1.22	3	-2.56	1.95	-22.69	1.46	-
$\frac{3}{2}(\frac{3}{2}^-)$	$\Sigma_b^* K^*$	4.73	1.46	4.37	0.64	3.91	-0.72	3.64	-1.81	3.33	-3.44	2.06	-27.95	1.46	-
$\frac{1}{2}(\frac{1}{2}^-)$	$\Sigma_b D^*$	3.11	1.46	2.93	1.05	2.7	0.36	2.56	-0.19	2.41	-1.02	1.76	-13.41	1.46	-
$\frac{3}{2}(\frac{1}{2}^-)$	$\Sigma_b D^*$	4.7	1.46	4.34	0.65	3.89	-0.69	3.62	-1.77	3.31	-3.39	2.05	-27.64	1.46	-
$\frac{1}{2}(\frac{3}{2}^-)$	$\Sigma_b D^*$	3.38	1.46	3.17	0.98	2.9	0.18	2.74	-0.46	2.56	-1.42	1.81	-15.83	1.46	-
$\frac{3}{2}(\frac{3}{2}^-)$	$\Sigma_b D^*$	4.33	1.46	4.01	0.75	3.61	-0.45	3.37	-1.4	3.1	-2.84	1.98	-24.33	1.46	-
$\frac{1}{2}(\frac{3}{2}^-)$	$\Sigma_b^* D^*$	3.54	1.46	3.31	0.94	3.02	0.08	2.85	-0.62	2.65	-1.66	1.84	-17.26	1.46	-
$\frac{3}{2}(\frac{3}{2}^-)$	$\Sigma_b^* D^*$	4.23	1.46	3.92	0.77	3.54	-0.38	3.31	-1.3	3.04	-2.69	1.96	-23.44	1.46	-

TABLE X: to be continued..

$I(J^P)$ State	Z=0		Z=0.2		Z=0.4		Z=0.5		Z=0.6		Z=0.9		Z=1	
	a_s	r_e	a_s	r_e	a_s	r_e	a_s	r_e	a_s	r_e	a_s	r_e	a_s	r_e
$1(1^-)$ $\Sigma_b B^*$	3.01	1.46	2.84	1.07	2.62	0.43	2.49	-0.09	2.35	-0.86	1.74	-12.47	1.46	-
$0(1^-)$ $\Sigma_b B^*$	4.24	1.46	3.93	0.77	3.54	-0.39	3.31	-1.32	3.05	-2.7	1.97	-23.53	1.46	-
$1(1^-)$ $\Sigma_b B^*$	3.13	1.46	2.94	1.05	2.71	0.35	2.57	-0.2	2.41	-1.04	1.76	-13.53	1.46	-
$0(1^-)$ $\Sigma_b B^*$	4.17	1.46	3.87	0.78	3.49	-0.34	3.27	-1.25	3.01	-2.6	1.95	-22.92	1.46	-
$2(1^-)$ $\Sigma_b^* B^*$	3.2	1.46	3.01	1.03	2.77	0.3	2.62	-0.28	2.46	-1.15	1.78	-14.19	1.46	-
$2(1^-)$ $\Sigma_b^* B^*$	4.13	1.46	3.83	0.8	3.46	-0.31	3.24	-1.2	2.98	-2.53	1.95	-22.51	1.46	-
$1(1^-)$ $\Xi_s K^*$	11.14	1.46	10.07	-0.96	8.72	-4.99	7.92	-8.22	6.99	-13.06	3.22	-85.67	1.46	-
$0(1^-)$ $\Xi_s K^*$	5.76	1.46	5.28	0.39	4.69	-1.4	4.33	-2.84	3.92	-4.99	2.24	-37.24	1.46	-
$1(1^-)$ $\Xi_s K^*$	8.57	1.46	7.78	-0.32	6.8	-3.28	6.2	-5.65	5.53	-9.2	2.75	-62.54	1.46	-
$0(1^-)$ $\Xi_s K^*$	7.25	1.46	6.61	0.01	5.81	-2.4	5.32	-4.33	4.77	-7.22	2.51	-50.66	1.46	-
$1(1^-)$ $\Xi_s K^*$	6.82	1.46	6.22	0.12	5.48	-2.11	5.03	-3.89	4.52	-6.57	2.44	-46.74	1.46	-
$1(1^-)$ $\Xi_s D^*$	6.59	1.46	6.02	0.18	5.31	-1.96	4.88	-3.67	4.39	-6.23	2.39	-44.71	1.46	-
$0(1^-)$ $\Xi_s D^*$	3.88	1.46	3.61	0.86	3.27	-0.15	3.07	-0.95	2.84	-2.16	1.9	-20.29	1.46	-
$1(1^-)$ $\Xi_s D^*$	5.99	1.46	5.49	0.33	4.86	-1.56	4.48	-3.07	4.05	-5.33	2.29	-39.29	1.46	-
$0(1^-)$ $\Xi_s D^*$	4.4	1.46	4.07	0.73	3.66	-0.49	3.42	-1.47	3.14	-2.94	2	-24.95	1.46	-
$1(1^-)$ $\Xi_s D^*$	5.48	1.46	5.04	0.46	4.48	-1.22	4.14	-2.56	3.76	-4.57	2.19	-34.73	1.46	-
$0(1^-)$ $\Xi_s B^*$	2.85	1.46	2.69	1.12	2.5	0.54	2.38	0.08	2.25	-0.61	1.71	-10.99	1.46	-
$1(1^-)$ $\Xi_s B^*$	5.26	1.46	4.84	0.51	4.31	-1.07	4	-2.34	3.63	-4.24	2.15	-32.74	1.46	-
$0(1^-)$ $\Xi_s B^*$	3.18	1.46	2.99	1.03	2.75	0.31	2.61	-0.26	2.45	-1.12	1.77	-14.02	1.46	-
$1(1^-)$ $\Xi_s B^*$	5.15	1.46	4.74	0.54	4.23	-0.99	3.92	-2.22	3.57	-4.06	2.13	-31.7	1.46	-
$0(1^-)$ $\Xi_s B^*$	3.28	1.46	3.07	1.01	2.82	0.25	2.67	-0.35	2.5	-1.26	1.79	-14.86	1.46	-
$1(1^-)$ $\Xi_s B^*$	4.98	1.46	4.59	0.58	4.1	-0.88	3.81	-2.06	3.47	-3.82	2.1	-30.2	1.46	-
$1(1^-)$ $\Xi_c K^*$	7.24	1.46	6.59	0.02	5.79	-2.39	5.31	-4.31	4.76	-7.2	2.51	-50.5	1.46	-
$0(1^-)$ $\Xi_c K^*$	4.17	1.46	3.87	0.78	3.49	-0.35	3.27	-1.25	3.01	-2.6	1.95	-22.93	1.46	-
$1(1^-)$ $\Xi_c K^*$	6.57	1.46	6	0.18	5.29	-1.94	4.87	-3.65	4.38	-6.2	2.39	-44.53	1.46	-
$0(1^-)$ $\Xi_c^* K^*$	4.84	1.46	4.47	0.62	4	-0.79	3.71	-1.92	3.39	-3.61	2.08	-28.95	1.46	-
$1(1^-)$ $\Xi_c^* K^*$	6.12	1.46	5.6	0.3	4.96	-1.64	4.57	-3.2	4.12	-5.53	2.31	-40.47	1.46	-
$1(1^-)$ $\Xi_c D^*$	5.9	1.46	5.41	0.35	4.79	-1.5	4.42	-2.97	4	-5.19	2.27	-38.47	1.46	-
$0(1^-)$ $\Xi_c D^*$	3.42	1.46	3.2	0.97	2.93	0.16	2.77	-0.5	2.58	-1.48	1.82	-16.16	1.46	-
$1(1^-)$ $\Xi_c D^*$	5.6	1.46	5.14	0.43	4.57	-1.3	4.22	-2.68	3.83	-4.75	2.21	-35.8	1.46	-
$0(1^-)$ $\Xi_c^* D^*$	3.76	1.46	3.51	0.89	3.19	-0.07	3	-0.84	2.78	-1.99	1.88	-19.25	1.46	-
$1(1^-)$ $\Xi_c^* D^*$	5.4	1.46	4.96	0.48	4.41	-1.16	4.09	-2.47	3.71	-4.44	2.18	-33.96	1.46	-
$0(1^-)$ $\Xi_c B^*$	2.72	1.46	2.58	1.15	2.41	0.62	2.3	0.2	2.18	-0.43	1.69	-9.9	1.46	-
$1(1^-)$ $\Xi_c B^*$	4.97	1.46	4.58	0.58	4.1	-0.88	3.8	-2.05	3.47	-3.81	2.1	-30.14	1.46	-
$0(1^-)$ $\Xi_c B^*$	2.94	1.46	2.78	1.09	2.57	0.48	2.45	-0.02	2.31	-0.75	1.73	-11.83	1.46	-
$1(1^-)$ $\Xi_c B^*$	4.89	1.46	4.51	0.6	4.04	-0.83	3.75	-1.97	3.42	-3.69	2.09	-29.43	1.46	-
$0(1^-)$ $\Xi_c^* B^*$	3.04	1.46	2.86	1.07	2.64	0.41	2.51	-0.11	2.36	-0.9	1.75	-12.71	1.46	-
$1(1^-)$ $\Xi_c^* B^*$	4.83	1.46	4.46	0.62	3.99	-0.78	3.71	-1.91	3.39	-3.59	2.07	-28.86	1.46	-

TABLE X: to be continued..

$I(J^P)$ State	Z=0		Z=0.2		Z=0.4		Z=0.5		Z=0.6		Z=0.9		Z=1	
	a_s	r_e	a_s	r_e	a_s	r_e	a_s	r_e	a_s	r_e	a_s	r_e	a_s	r_e
$0(\frac{1}{2}^-)$ $\Xi_b K^*$	3.08	1.46	2.9	1.06	2.68	0.38	2.54	-0.16	2.39	-0.97	1.76	-13.13	1.46	-
$1(\frac{1}{2}^-)$ $\Xi_b K^*$	5.7	1.46	5.23	0.4	4.64	-1.36	4.29	-2.77	3.88	-4.89	2.23	-36.66	1.46	-
$0(\frac{3}{2}^-)$ $\Xi_b K^*$	3.44	1.46	3.22	0.97	2.94	0.15	2.78	-0.51	2.59	-1.5	1.82	-16.31	1.46	-
$1(\frac{3}{2}^-)$ $\Xi_b K^*$	5.57	1.46	5.11	0.43	4.54	-1.28	4.2	-2.65	3.81	-4.7	2.21	-35.52	1.46	-
$0(\frac{1}{2}^-)$ $\Xi_b D^*$	2.77	1.46	2.62	1.14	2.44	0.59	2.33	0.16	2.21	-0.5	1.7	-10.29	1.46	-
$1(\frac{1}{2}^-)$ $\Xi_b D^*$	5.02	1.46	4.62	0.57	4.13	-0.91	3.83	-2.1	3.5	-3.88	2.11	-30.56	1.46	-
$0(\frac{3}{2}^-)$ $\Xi_b D^*$	2.99	1.46	2.82	1.08	2.61	0.44	2.48	-0.06	2.33	-0.83	1.74	-12.27	1.46	-
$1(\frac{3}{2}^-)$ $\Xi_b D^*$	4.94	1.46	4.55	0.59	4.07	-0.86	3.78	-2.02	3.45	-3.76	2.09	-29.84	1.46	-
$0(\frac{1}{2}^-)$ $\Xi_b B^*$	2.67	1.46	2.53	1.16	2.36	0.66	2.26	0.26	2.15	-0.34	1.68	-9.37	1.46	-
$1(\frac{1}{2}^-)$ $\Xi_b B^*$	4.85	1.46	4.48	0.61	4.01	-0.8	3.72	-1.93	3.4	-3.62	2.08	-29.06	1.46	-
$0(\frac{3}{2}^-)$ $\Xi_b B^*$	2.76	1.46	2.61	1.14	2.43	0.6	2.33	0.17	2.2	-0.48	1.7	-10.2	1.46	-
$1(\frac{3}{2}^-)$ $\Xi_b B^*$	4.82	1.46	4.44	0.62	3.98	-0.77	3.7	-1.89	3.38	-3.57	2.07	-28.72	1.46	-

Appendix A: s-wave OBE potential and net effective potential

It is interesting to see the s-wave one meson exchange contribution to the OBE interaction potential, which is shown in the Fig-6 when effective s-wave OBE, Yukawa-like screen and net effective potential shown in Fig-7. The graphs are plotted for all possible isospin-spin channels.

We can see from Fig-6 that in all possible isospin-spin channels, the s-wave σ -exchange potential is an attractive in nature while the s-wave ω -exchange is repulsive.

The behavior of s-wave π -exchange potential is repulsive in (I,S)=(1/2, 1/2) and (3/2, 5/2) channels when it is an attractive in other channels, moreover it seems relatively strong attractive in (I,S)=(1/2, 5/2) channel.

We can see from the figure that the strength of the s-wave η and ρ meson exchange are relatively weak. However, the η -exchange is an attractive in (I,S)=(1/2, 1/2), (3/2, 1/2) and (1/2, 3/2) channels while ρ -exchange is an attractive in (3/2, 1/2), (1/2, 3/2) and (1/2, 5/2) channels.

The scalar s-wave δ -exchange (which is also known as

a_0 -exchange) is attractive in (I,S)=(3/2, 1/2), (3/2, 3/2) and (3/2, 5/2) channels while its strength is seems relatively weak compared to s-wave σ -exchange.

From Fig-7, we can see the behavior of the net s-wave OBE potential, Yukawa-like screen potential and net effective potential in possible isospin-spin channels.

It can be seen from Fig-7 that the strength of the net effective potential highly influenced by attractive Yukawa-like potential.

The effective s-wave OBE gets attractive in (I,S)=(1/2, 5/2), (1/2, 3/2) and (3/2, 1/2) channels, in which (1/2, 5/2) channel get more attractive depth than (1/2, 3/2) channel while channel (3/2, 1/2) being the weakest attractive channel.

However, these attractive channels of s-wave OBE get depth around 4-6 fm.

Thus, even pure s-wave OBE have a possibilities of shallow bound states in these particular channels.

Moreover, the attractive Yukawa-like potential have shown high impact on net effective interaction potential which reflect in the calculated results.

-
- [1] D.P. Rathaud, A.K. Rai (2017), 1706.09323
 - [2] R. Aaij et al. (LHCb Collaboration), Phys. Rev. Lett. **115**, 072001 (2015)
 - [3] M. Gell-Mann, Physics Letters **8**, 214 (1964)
 - [4] R.J. Jaffe, Phys. Rev. D **15**, 267 (1977)
 - [5] D. Strottman, Phys. Rev. D **20**, 748 (1979)
 - [6] H.J. Lipkin, Physics Letters B **195**, 484 (1987)
 - [7] T. Nakano et al., Phys. Rev. Lett. **91**, 012002 (2003)
 - [8] V.V. Barmin et al., Physics of Atomic Nuclei **66**, 1715 (2003)
 - [9] S. Stepanyan et al. (CLAS Collaboration), Phys. Rev. Lett. **91**, 252001 (2003)
 - [10] A. Aktas et al., Physics Letters B **588**, 17 (2004)
 - [11] I. Abt et al. (HERA-B Collaboration), Phys. Rev. Lett. **93**, 212003 (2004)
 - [12] K.T. Knpfle et al., Journal of Physics G: Nuclear and Particle Physics **30**, S1363 (2004)
 - [13] J.Z. Bai et al. (BES Collaboration), Phys. Rev. D **70**, 012004 (2004)
 - [14] B. Aubert et al. (BABAR Collaboration), Phys. Rev. D

- 76**, 092004 (2007)
- [15] J. Link et al., *Physics Letters B* **622**, 229 (2005)
- [16] M. Moritsu et al. (J-PARC E19 Collaboration), *Phys. Rev. C* **90**, 035205 (2014)
- [17] B. Abelev et al. (ALICE Collaboration), *The European Physical Journal C* **75**, 1 (2015)
- [18] G.N. Li, X.G. He, M. He, *Journal of High Energy Physics* **2015**, 1 (2015)
- [19] R.F. Lebed, *Physics Letters B* **749**, 454 (2015)
- [20] L. Maiani, A. Polosa, V. Riquer, *Physics Letters B* **749**, 289 (2015)
- [21] Z.G. Wang, *The European Physical Journal C* **76**, 70 (2016)
- [22] R. Chen, X. Liu, S.L. Zhu, *Nuclear Physics A* **954**, 406 (2016), recent Progress in Strangeness and Charm Hadronic and Nuclear Physics
- [23] R. Chen, J. He, X. Liu, *Chinese Physics C* **41**, 103105 (2017)
- [24] K. Azizi, Y. Sarac, H. Sundu, *Phys. Rev. D* **96**, 094030 (2017)
- [25] K. Azizi, Y. Sarac, H. Sundu, *Phys. Rev. D* **95**, 094016 (2017)
- [26] C.W. Shen, Y.H. Lin (2017), 1710.09037
- [27] N.N. Scoccola, D.O. Riska, M. Rho, *Phys. Rev. D* **92**, 051501 (2015)
- [28] F.K. Guo et al., *Phys. Rev. D* **92**, 071502 (2015)
- [29] F.K. Guo et al., *The European Physical Journal A* **52**, 318 (2016)
- [30] U.G. Meiner, J. Oller, *Physics Letters B* **751**, 59 (2015)
- [31] X.H. Liu, Q. Wang, Q. Zhao, *Physics Letters B* **757**, 231 (2016)
- [32] M.I. Eides, V.Y. Petrov, M.V. Polyakov, *The European Physical Journal C* **78**, 36 (2018)
- [33] H.X. Chen et al., *Physics Reports* **639**, 1 (2016), the hidden-charm pentaquark and tetraquark states
- [34] E.S. Swanson, *Physics Reports* **429**, 243 (2006)
- [35] A. Esposito, A. Pilloni, A. Polosa, *Physics Reports* **668**, 1 (2017)
- [36] A. Ali, J.S. Lange, S. Stone, *Progress in Particle and Nuclear Physics* **97**, 123 (2017)
- [37] F.K. Guo et al., *Rev. Mod. Phys.* **90**, 015004 (2018)
- [38] R. Machleidt, K. Holinde, C. Elster, *Physics Reports* **149**, 1 (1987)
- [39] N. Lee et al., *Phys. Rev. D* **84**, 014031 (2011)
- [40] G.J. Ding, J.F. Liu, M.L. Yan, *Phys. Rev. D* **79**, 054005 (2009)
- [41] A.K. Rai, D.P. Rathaud, *Eur. Phys. J. C* **75**, 462 (2015)
- [42] D.P. Rathaud, A.K. Rai, *The European Physical Journal Plus* **132**, 370 (2017)
- [43] D.P. Rathaud, A.K. Rai, *Indian J. Phys.* **90**, 1299 (2016)
- [44] D. Ebert, R.N. Faustov, V.O. Galkin, *Phys. Rev. D* **79**, 114029 (2009)
- [45] A.M. Badalian, A.I. Veselov, B.L.G. Bakker, *Phys. Rev. D* **70**, 016007 (2004)
- [46] R. Machleidt, *Phys. Rev. C* **63**, 024001 (2001)
- [47] C. Patrignani et al. (Particle Data Group), *Chin. Phys. C* **40**, 100001 (2016)
- [48] M.W. Paris, V.R. Pandharipande, *Phys. Rev. C* **62**, 015201 (2000)
- [49] M. Naghdi, *Physics of Particles and Nuclei* **45**, 924 (2014)
- [50] J.J. Wu et al., *Phys. Rev. C* **84**, 015202 (2011)
- [51] S. Weinberg, *Phys. Rev.* **137**, B672 (1965)

FIG. 6: The characteristic nature of the individual s-wave meson exchange potential, in a respective isospin-spin channels. The graphs are plotted for the $\Sigma_{s,c,b} - D^*$ systems. These graphs can be consider as generalize plots to understand the behavior of the potentials in respective isospin-spin channels for other systems, as the similar nature have been found in different meson-baryon systems with small scaling.

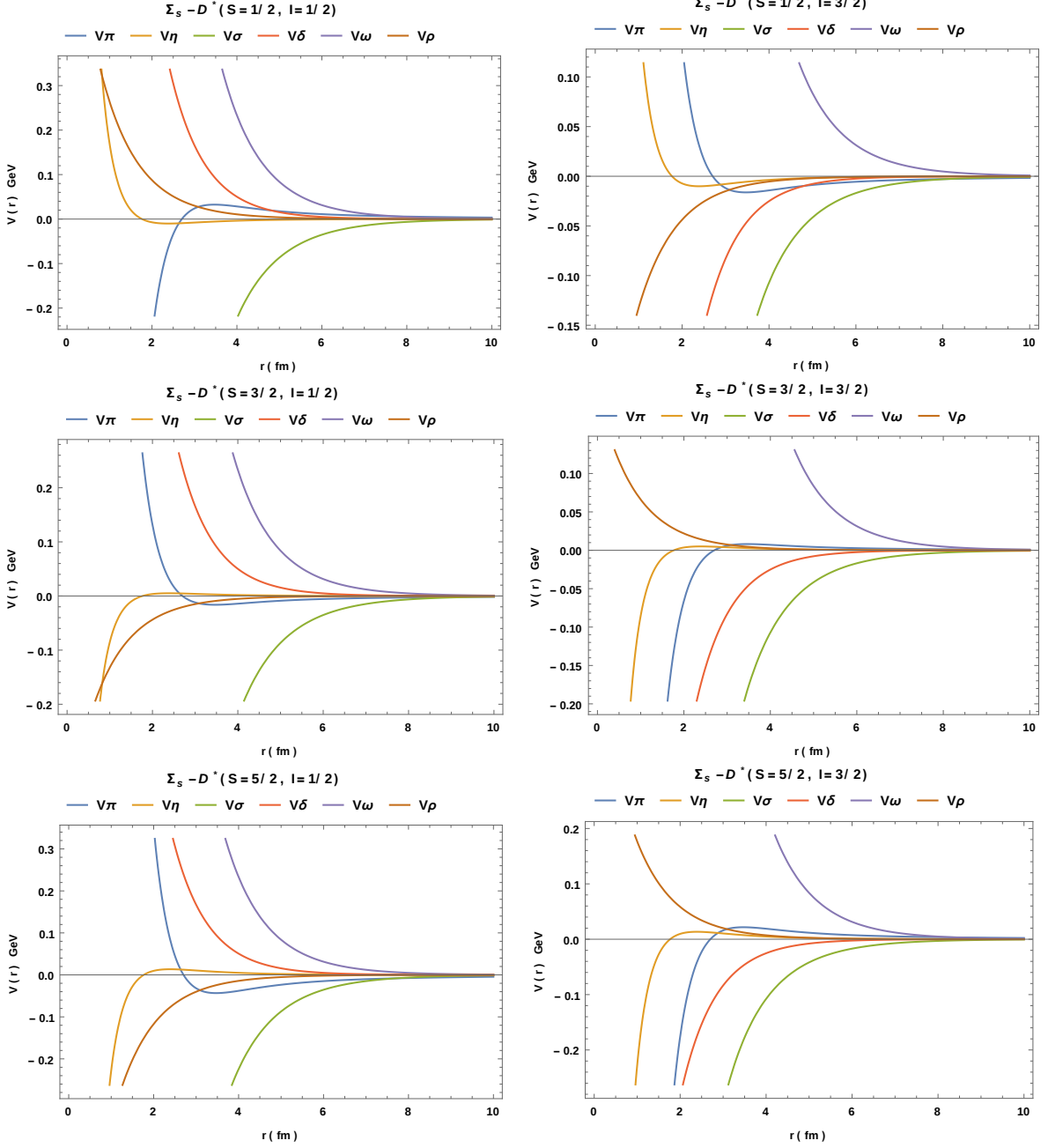


FIG. 6: to be continued..

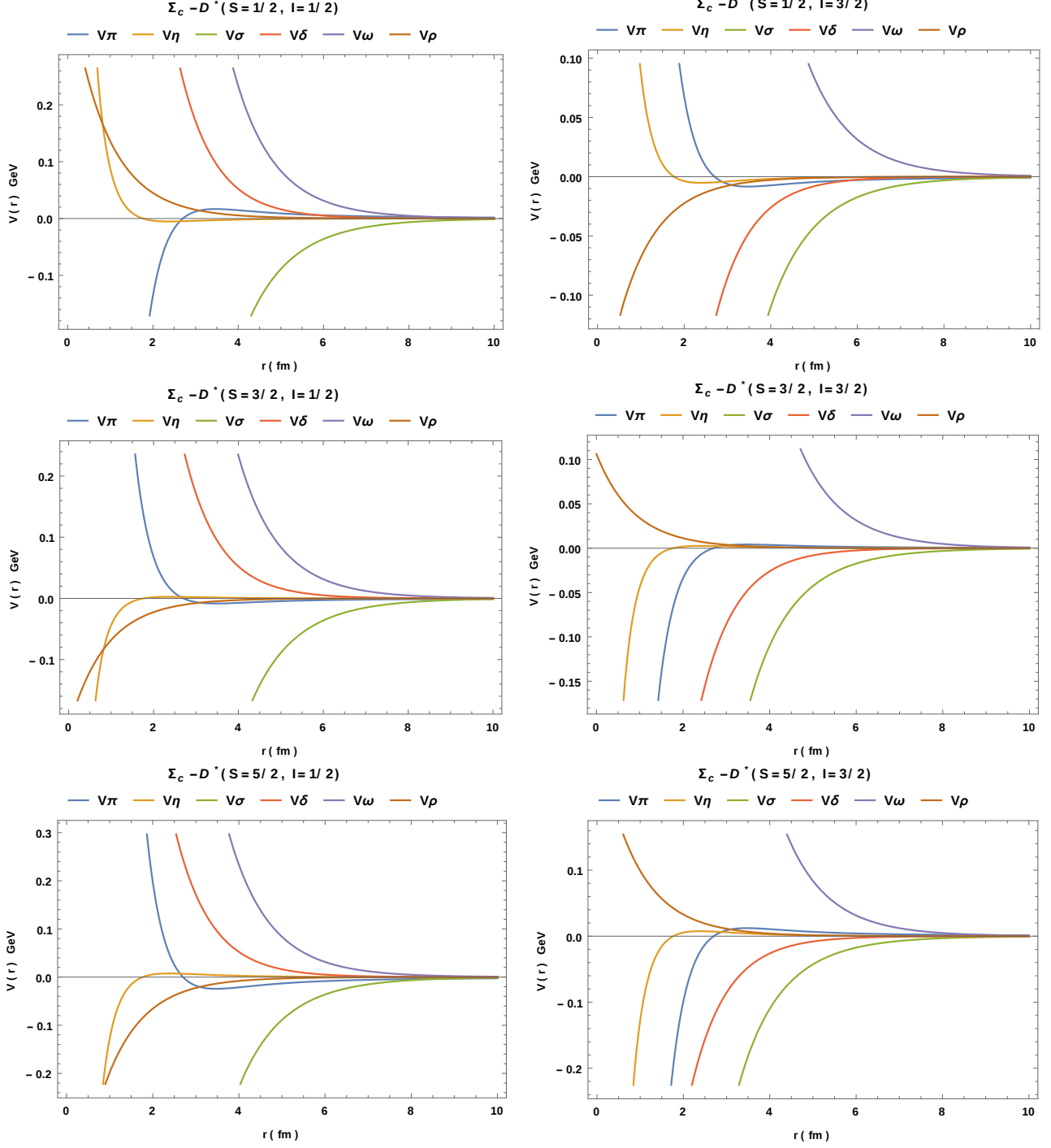


FIG. 6: to be continued..

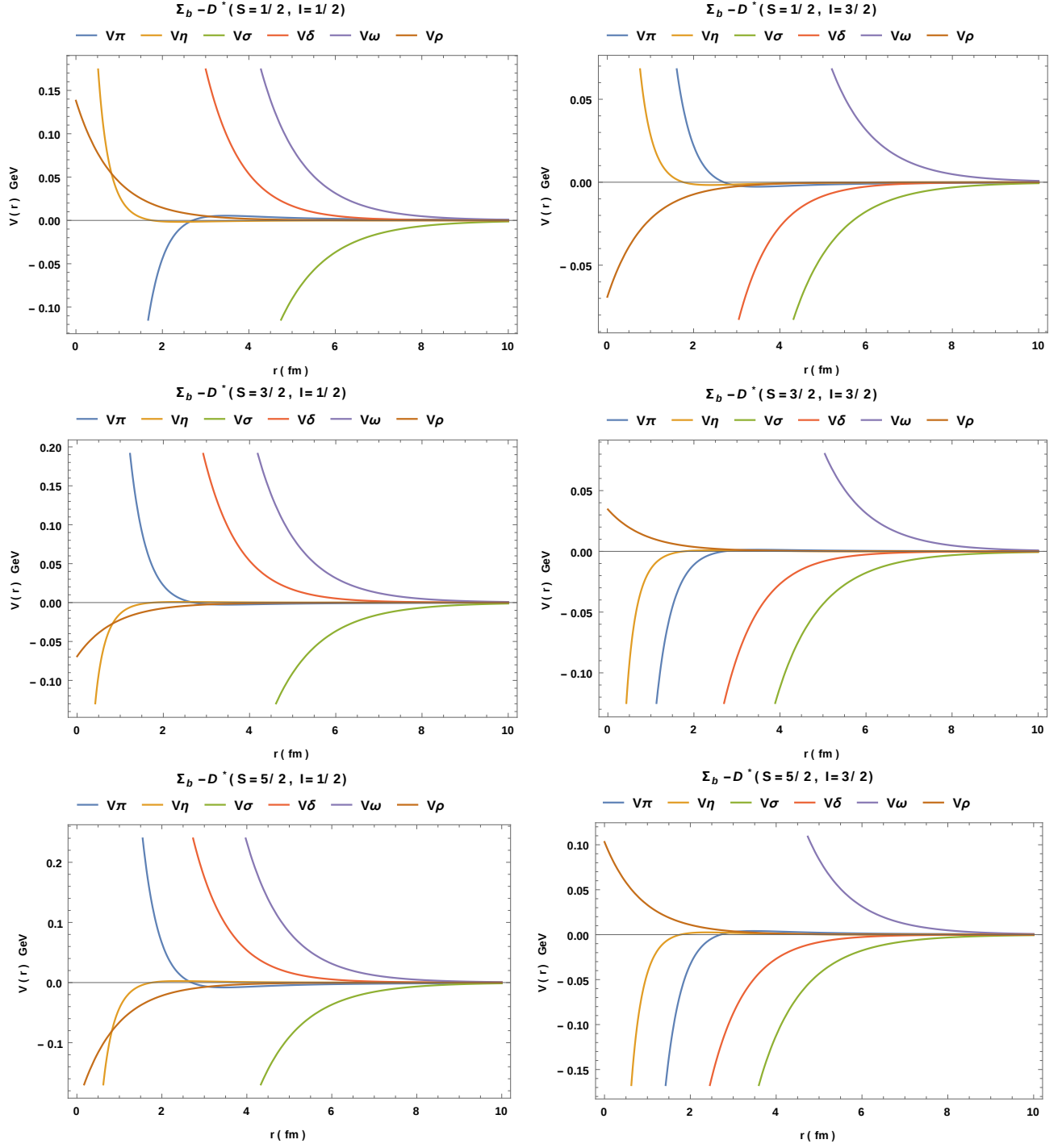


FIG. 7: The contributory nature of the s-wave OBE potential (V_{obe}), Yukawa-like screen potential (V_y) and net effective potential ($V_{eff} = V_{obe} + V_y$) in a respective isospin-spin channels are shown. The graphs are plotted for the $\Sigma_{s,c,b} - D^*$ systems. These graphs can be consider as generalize plots to understand the behavior of the potentials in respective isospin-spin channels for other systems, as the similar nature have been found in different meson-baryon systems with small scaling.

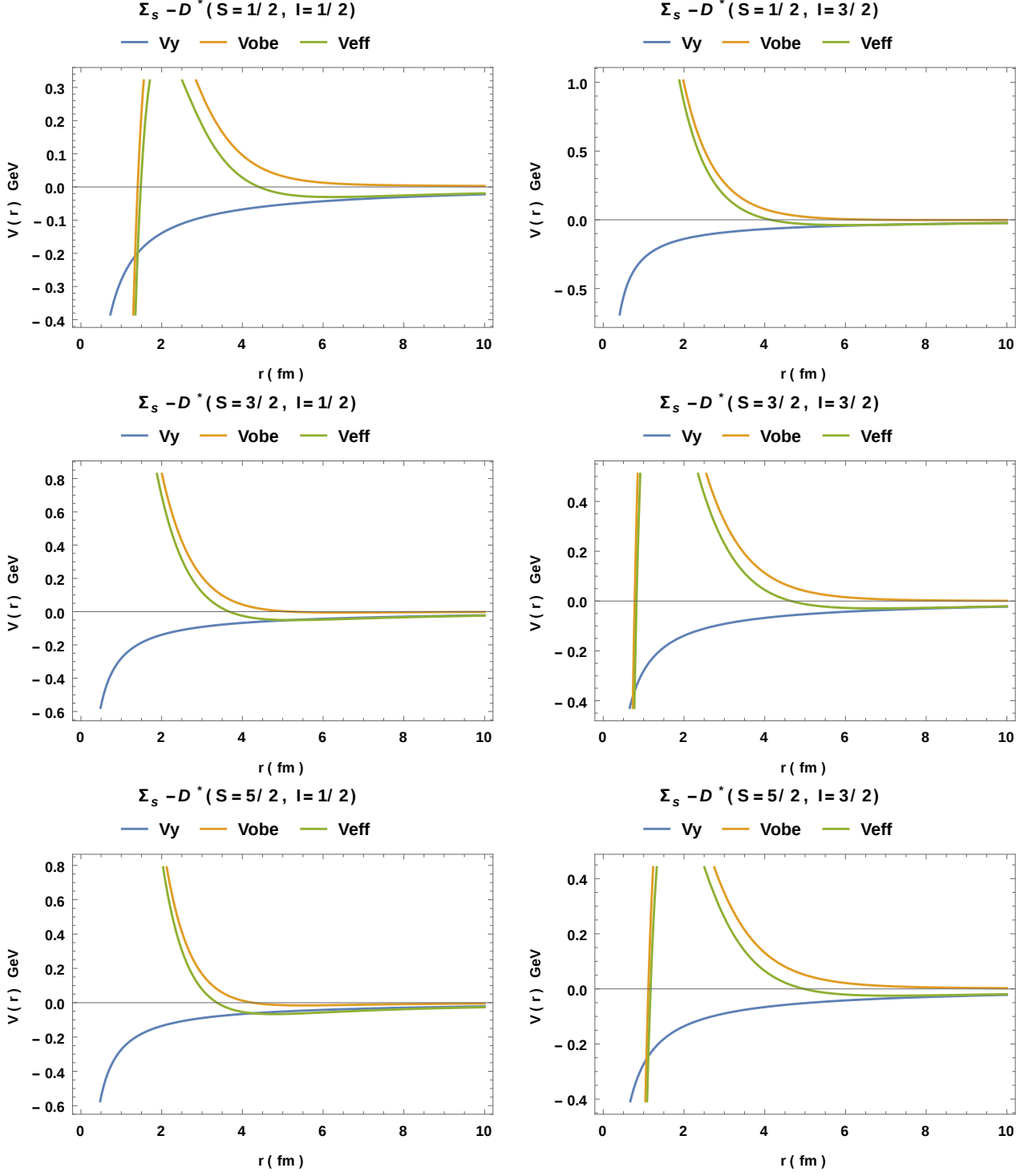


FIG. 7: to be continued..

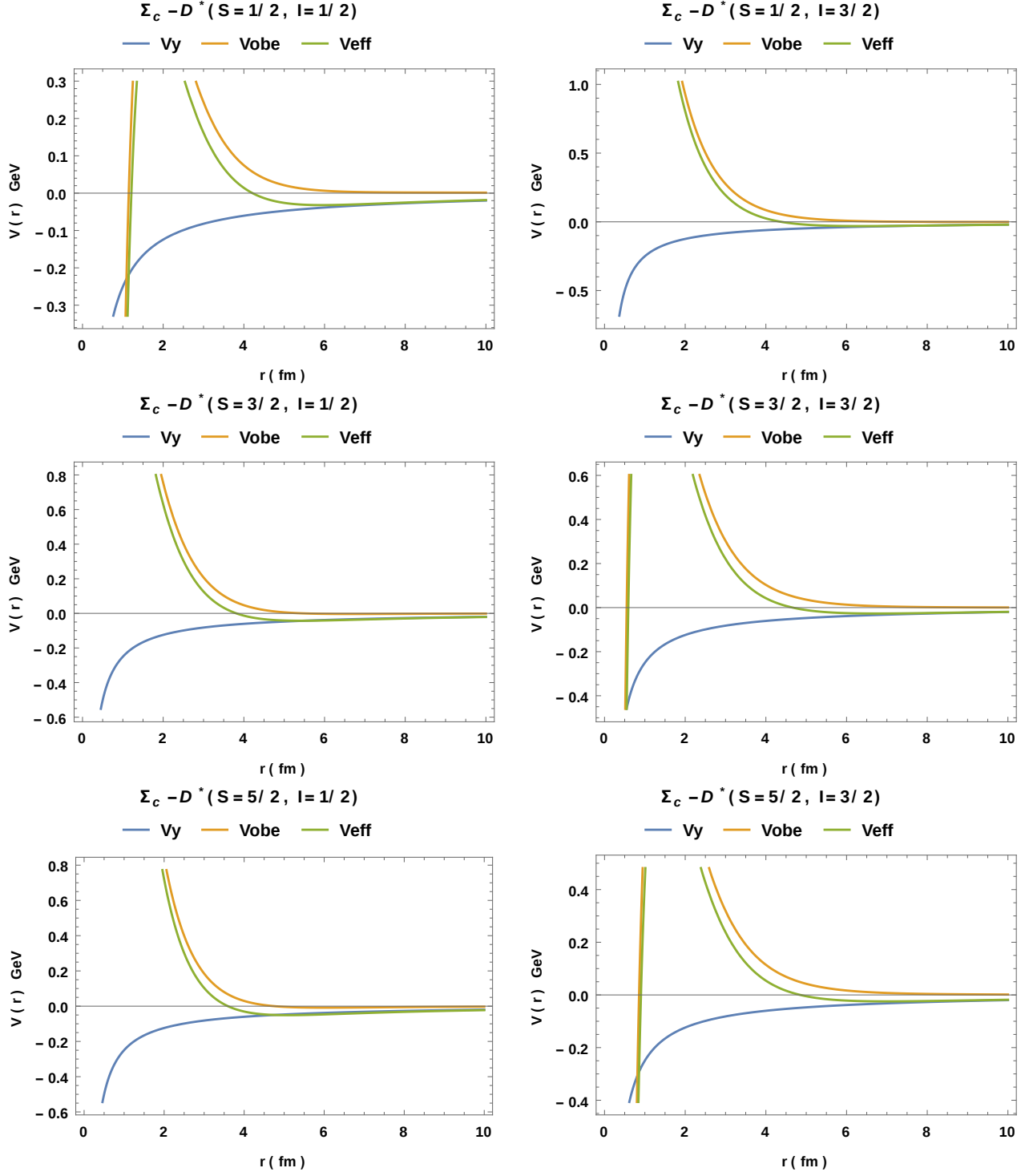


FIG. 7: to be continued..

